Searching Ultralight Axions with Quantum Technology

M. Bauer, *SC* and G. Rostagni, [arXiv:2408.06412 [hep-ph] , JHEP 0X (2025) XXX]
M. Bauer and *SC*, [arXiv:2408.06408 [hep-ph]]

HECA seminar @ University of Warsaw & NCNR
April 29, 2025

Sreemanti Chakraborti

Durham University

IP3

Dark matter

*Compelling evidence **(only gravitational)** of non-luminous matter*

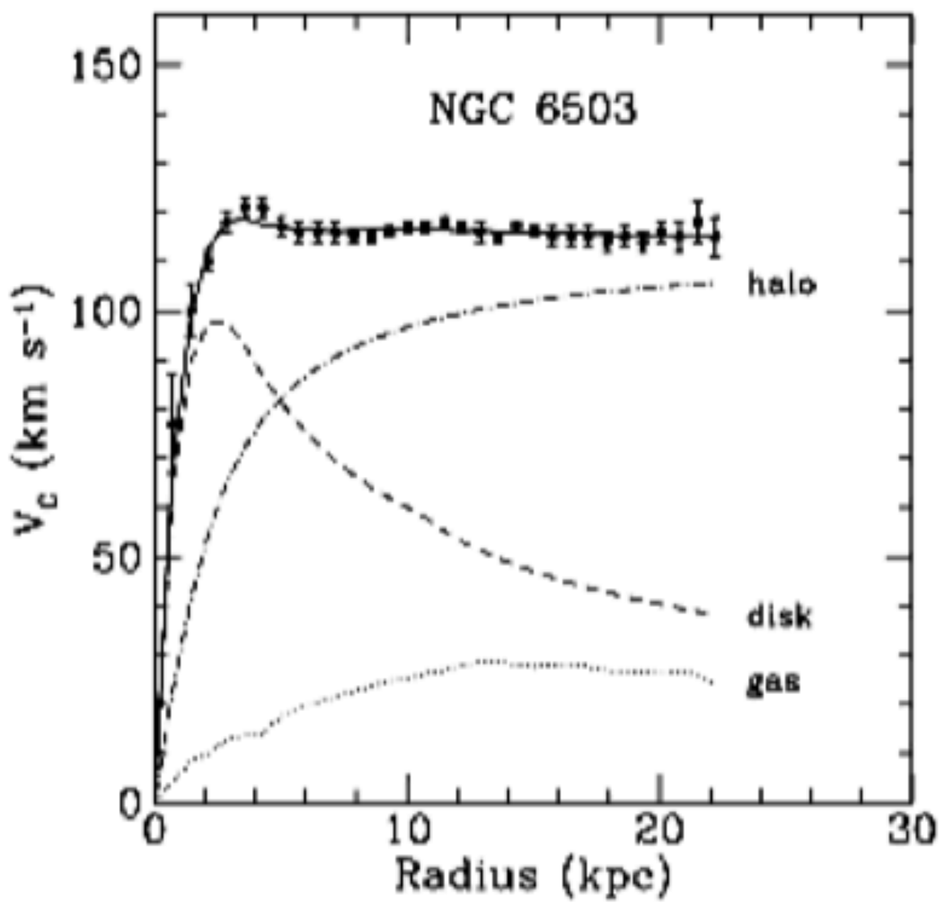

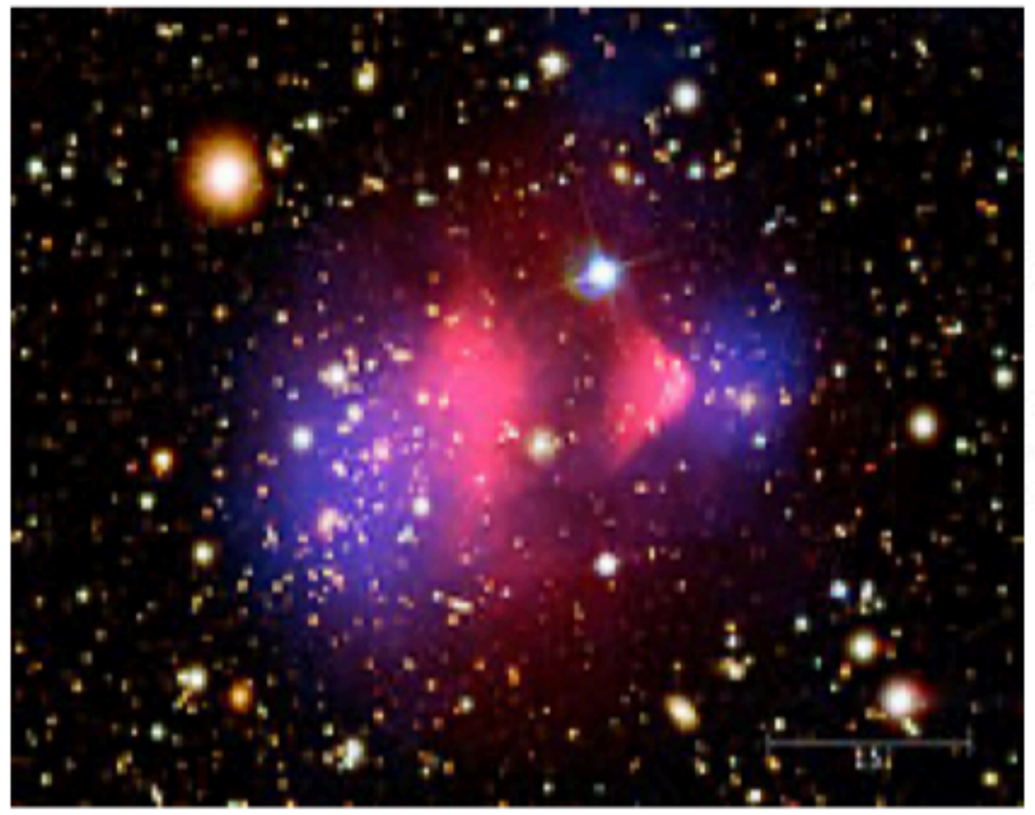

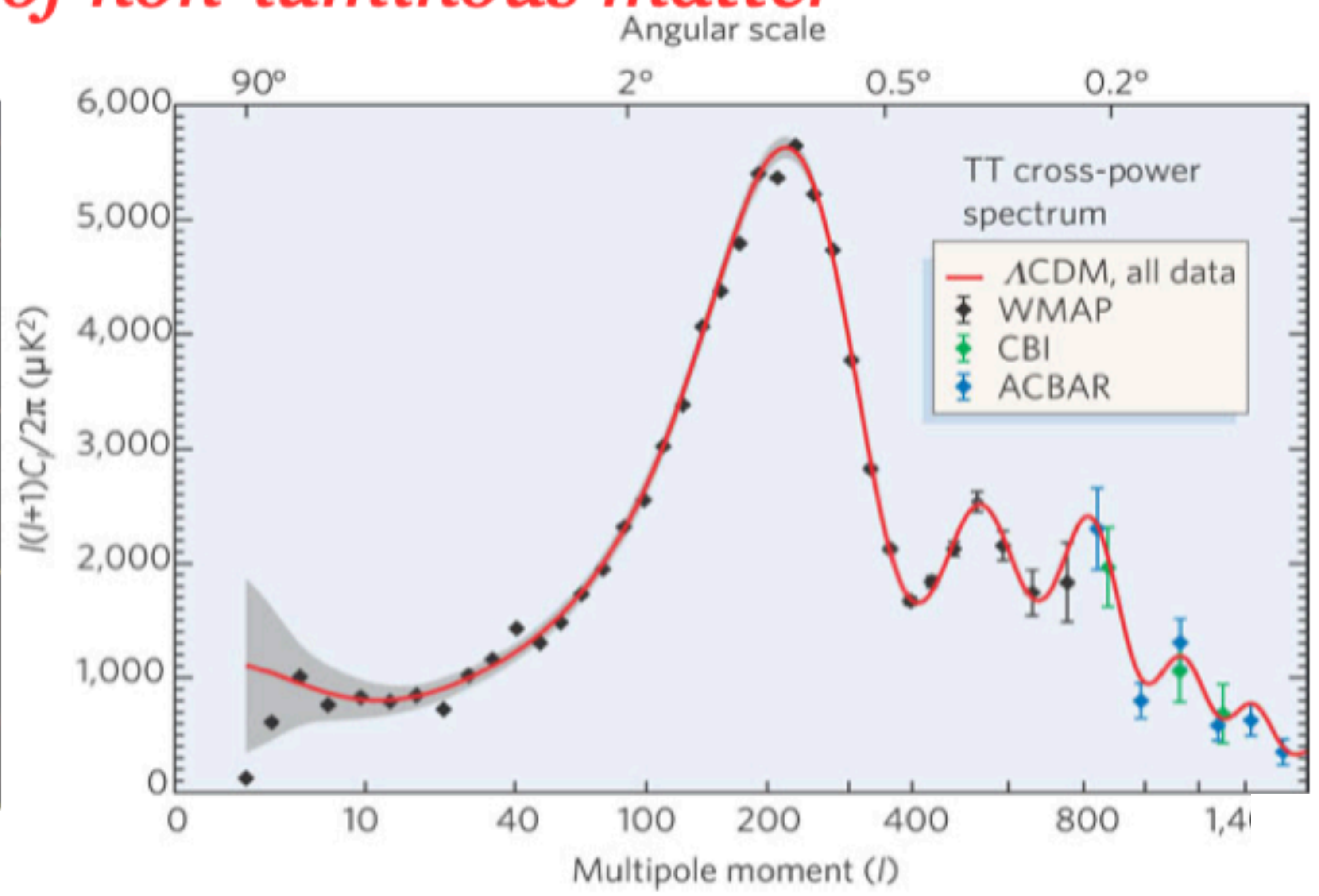

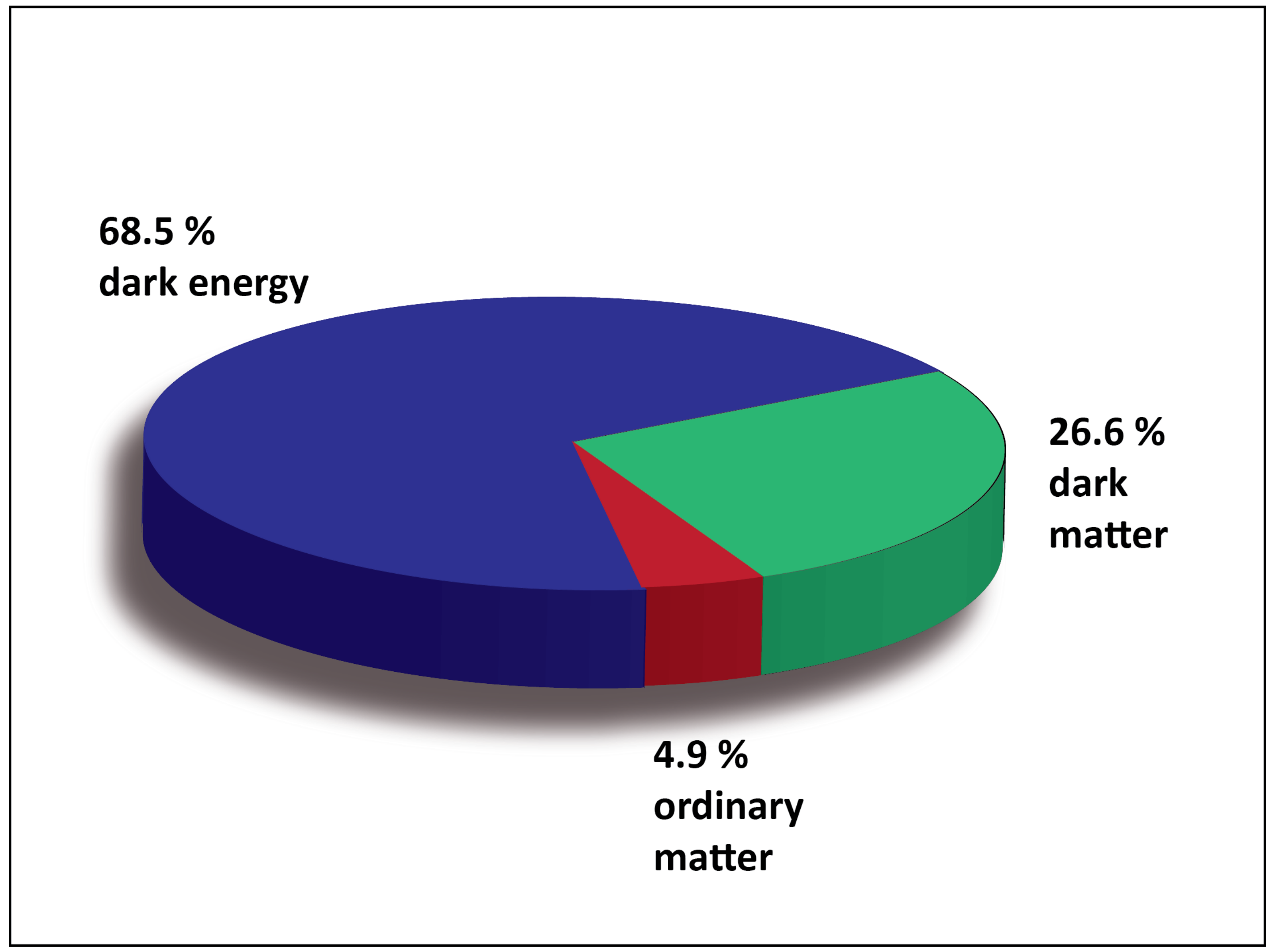

We know...

- its abundance
- presureless
- long-lived enough
- neutral enough

We don't know...

- fundamental particle?
- spin, mass?
- non-gravitational interactions?
- **thermal relic?**
- when was it produced?
- ...

$$\rho_{\rm DM}^{\rm local} \approx 0.4\,{\rm GeV/cm^3}$$

$$v_{\rm DM} \sim 300\ {\rm km/s}$$

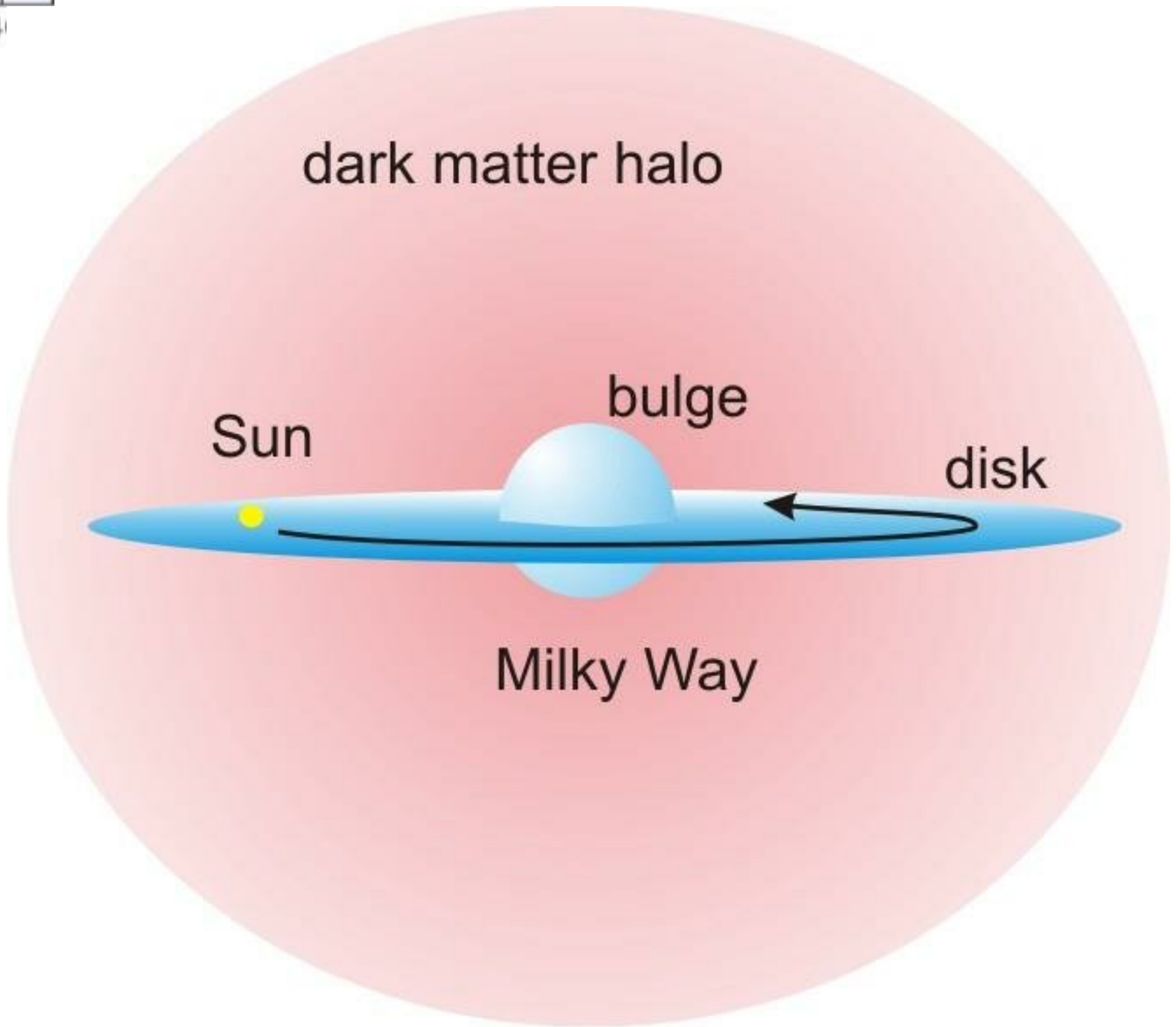

Dark matter on the mass scale

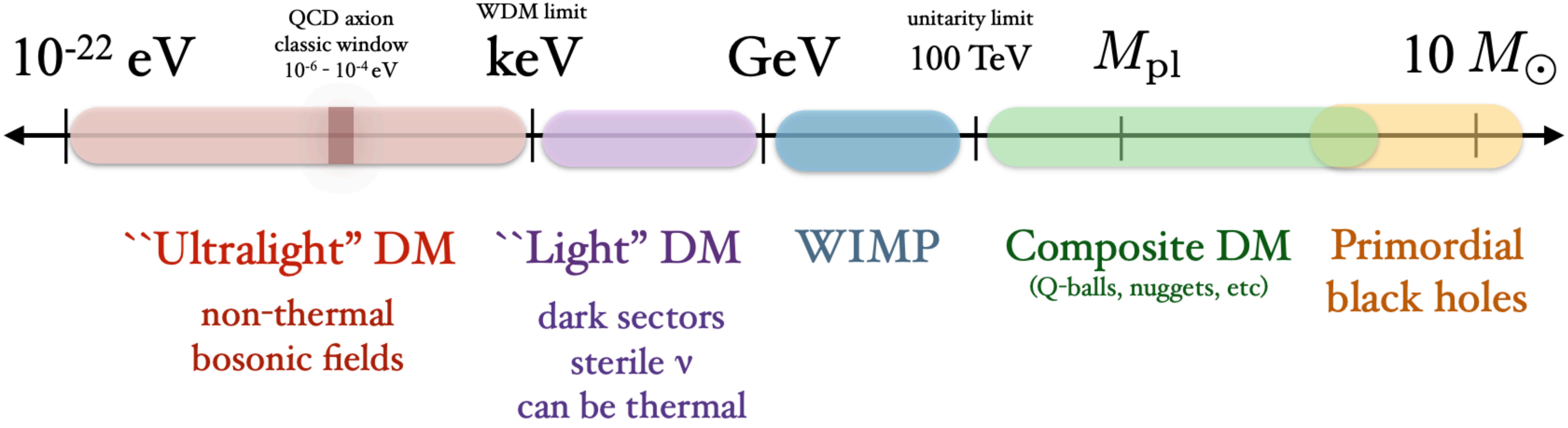

Traditional searches for particle dark matter

Thermal WIMPs

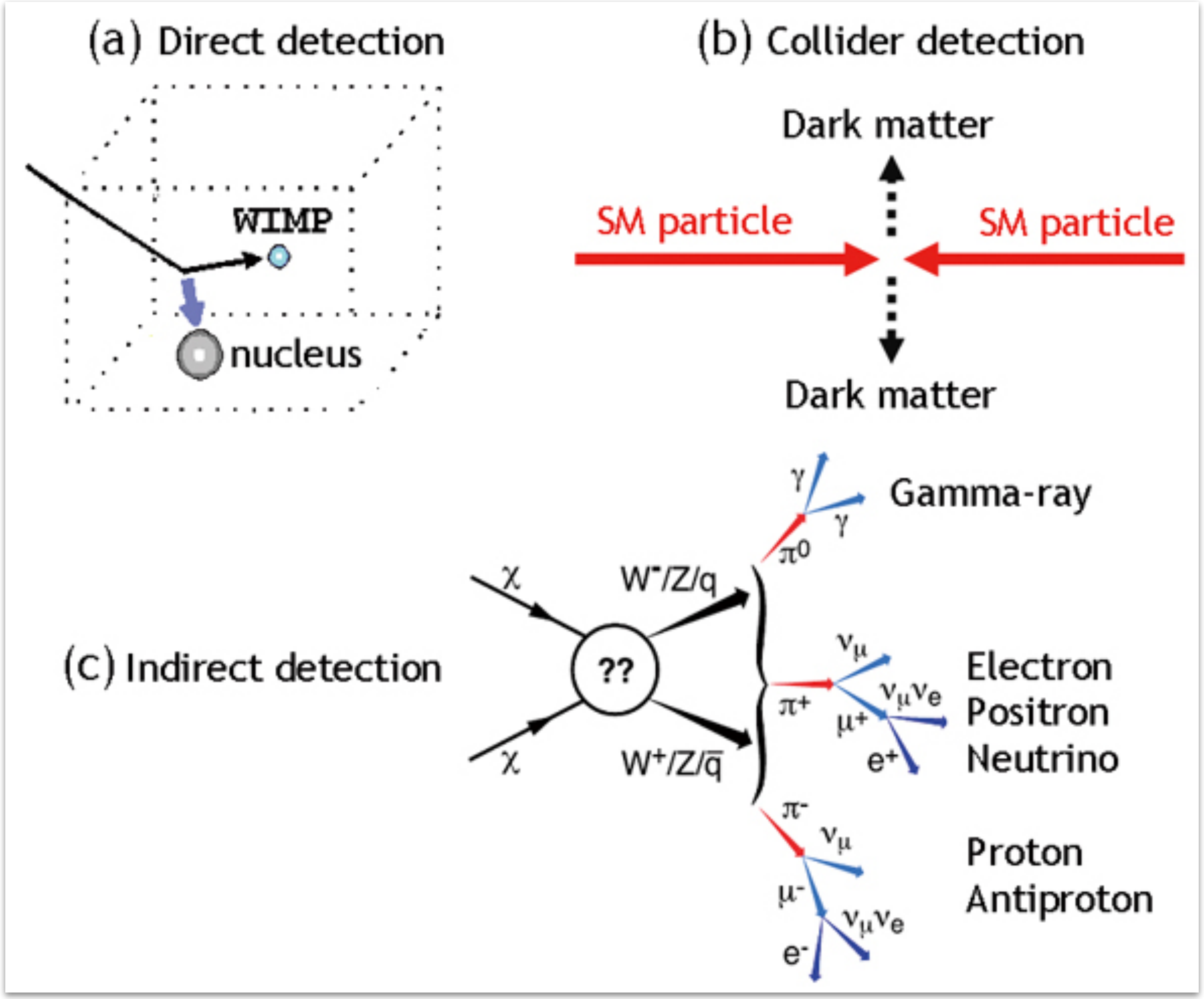

Traditional searches for particle dark matter

Thermal WIMPs

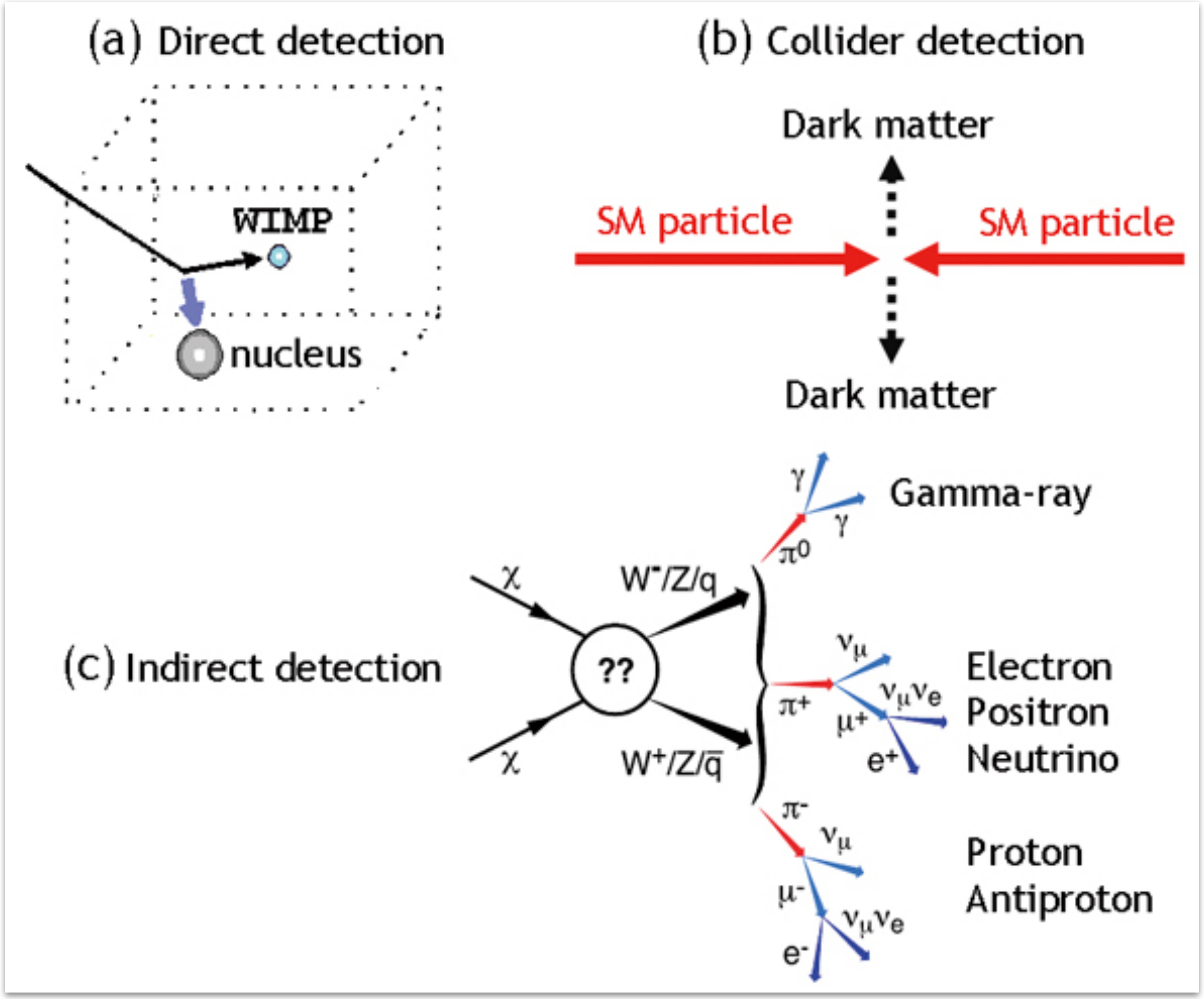

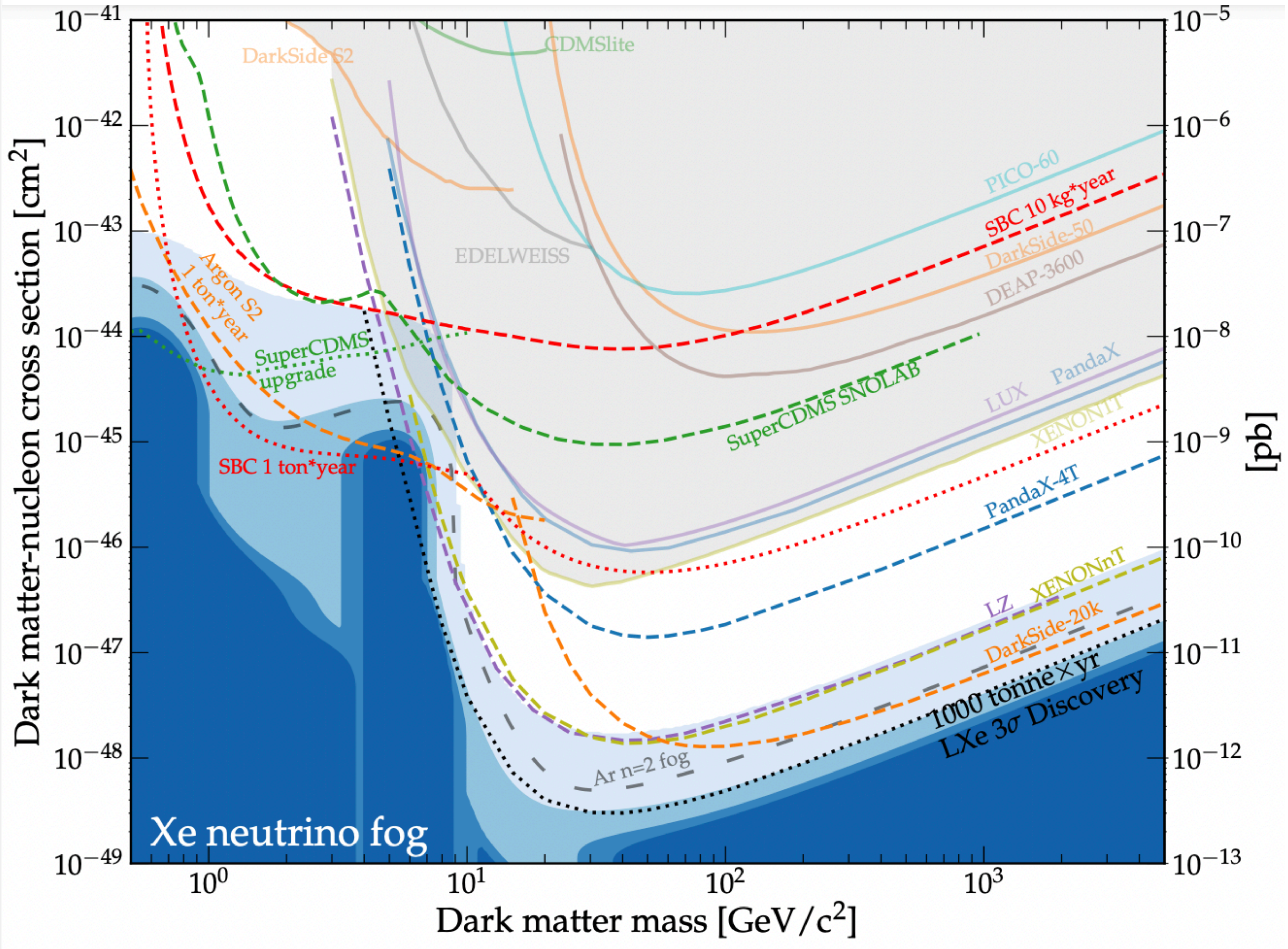

Snowmass 2021 Cosmic Frontier : 2203.08084

WIMP landscape

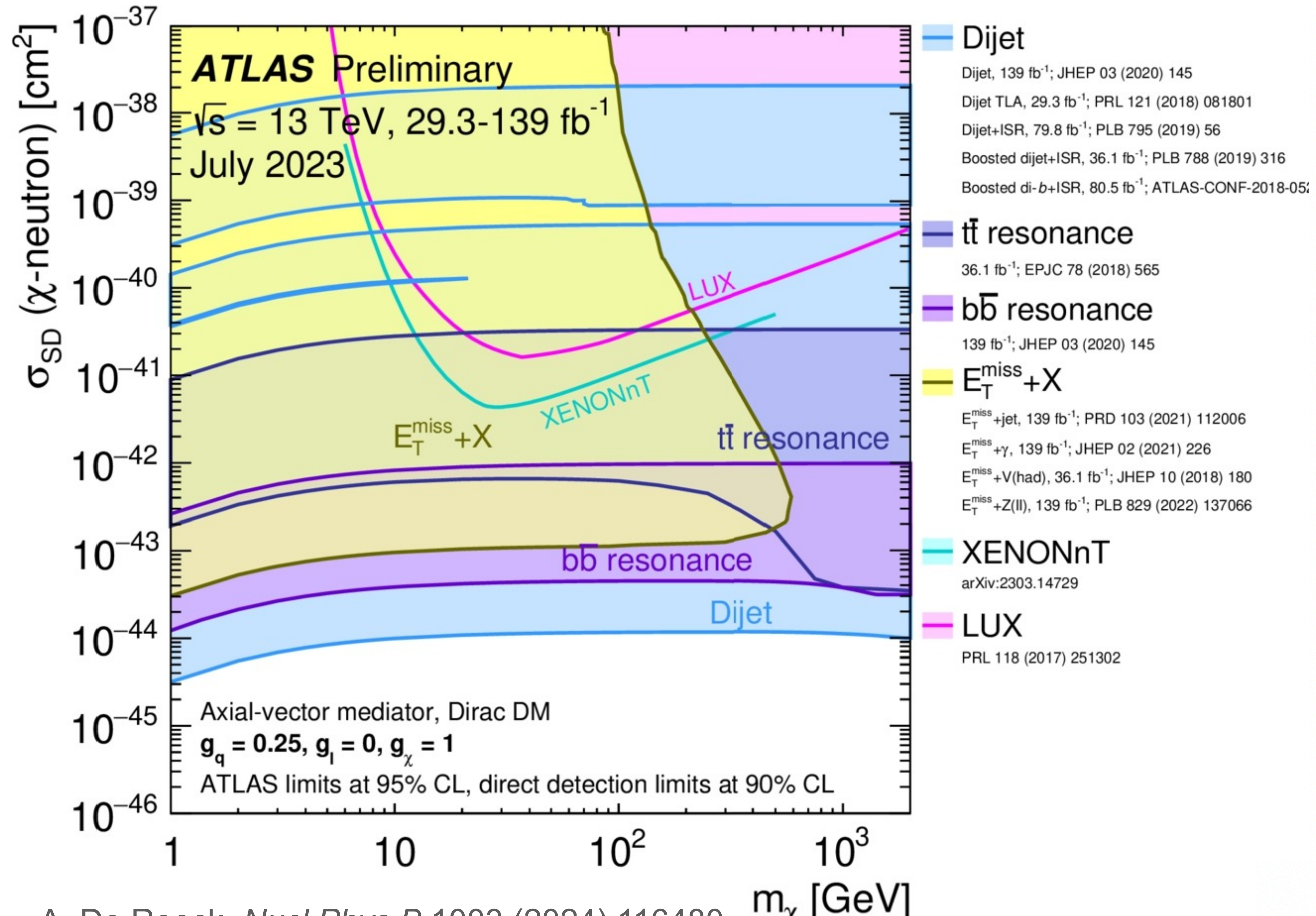

A. De Roeck, *Nucl.Phys.B* 1003 (2024) 116480

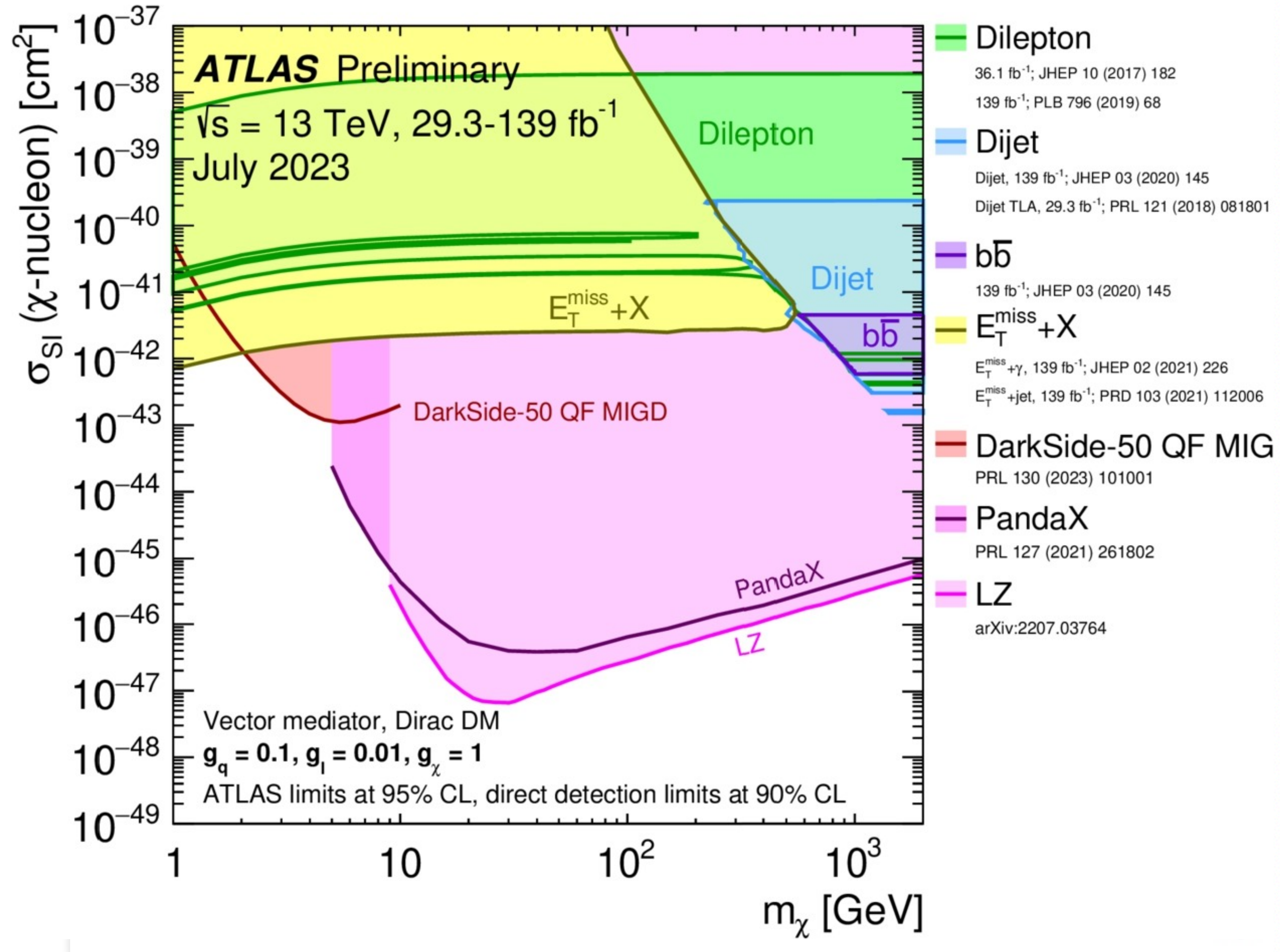

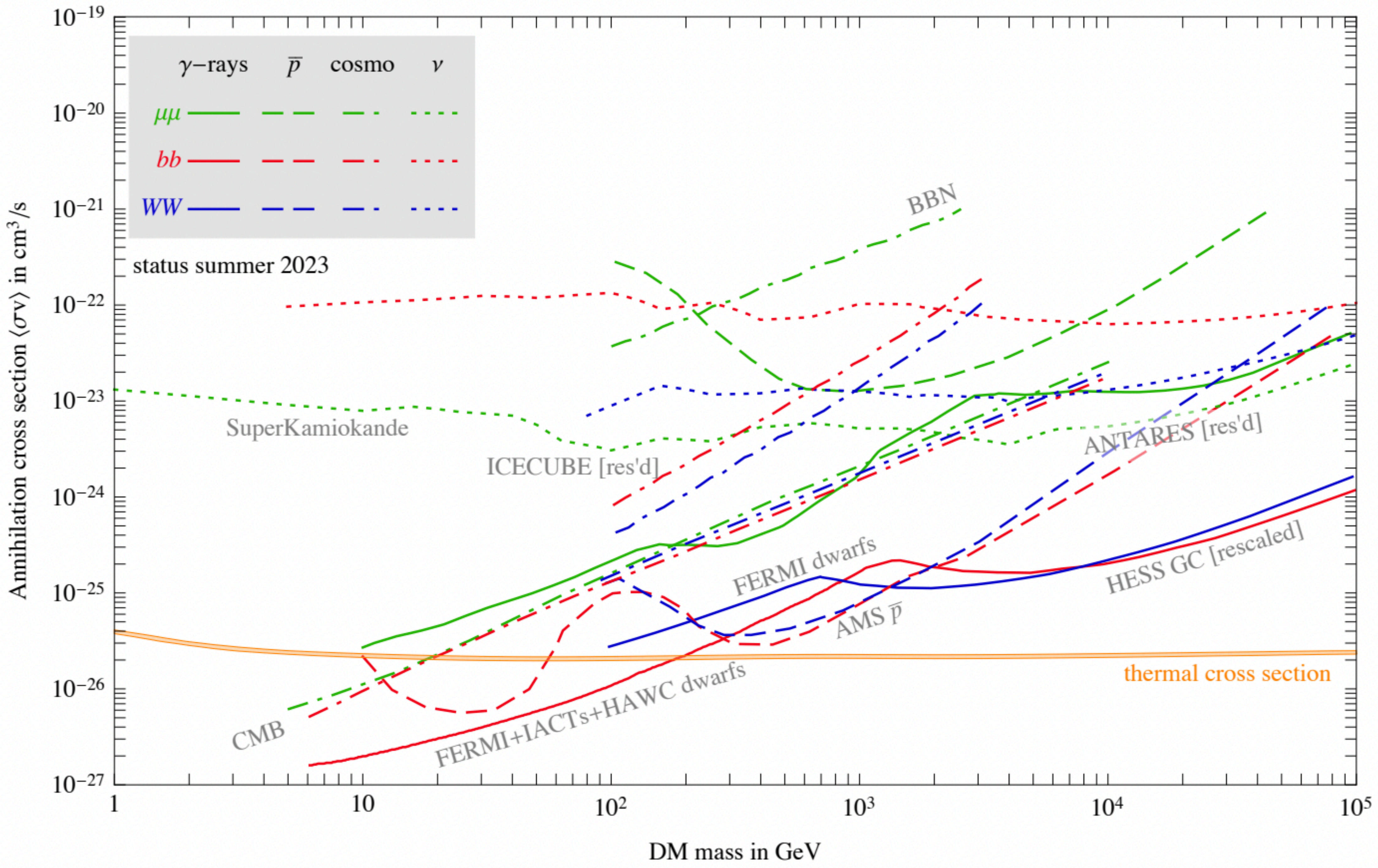

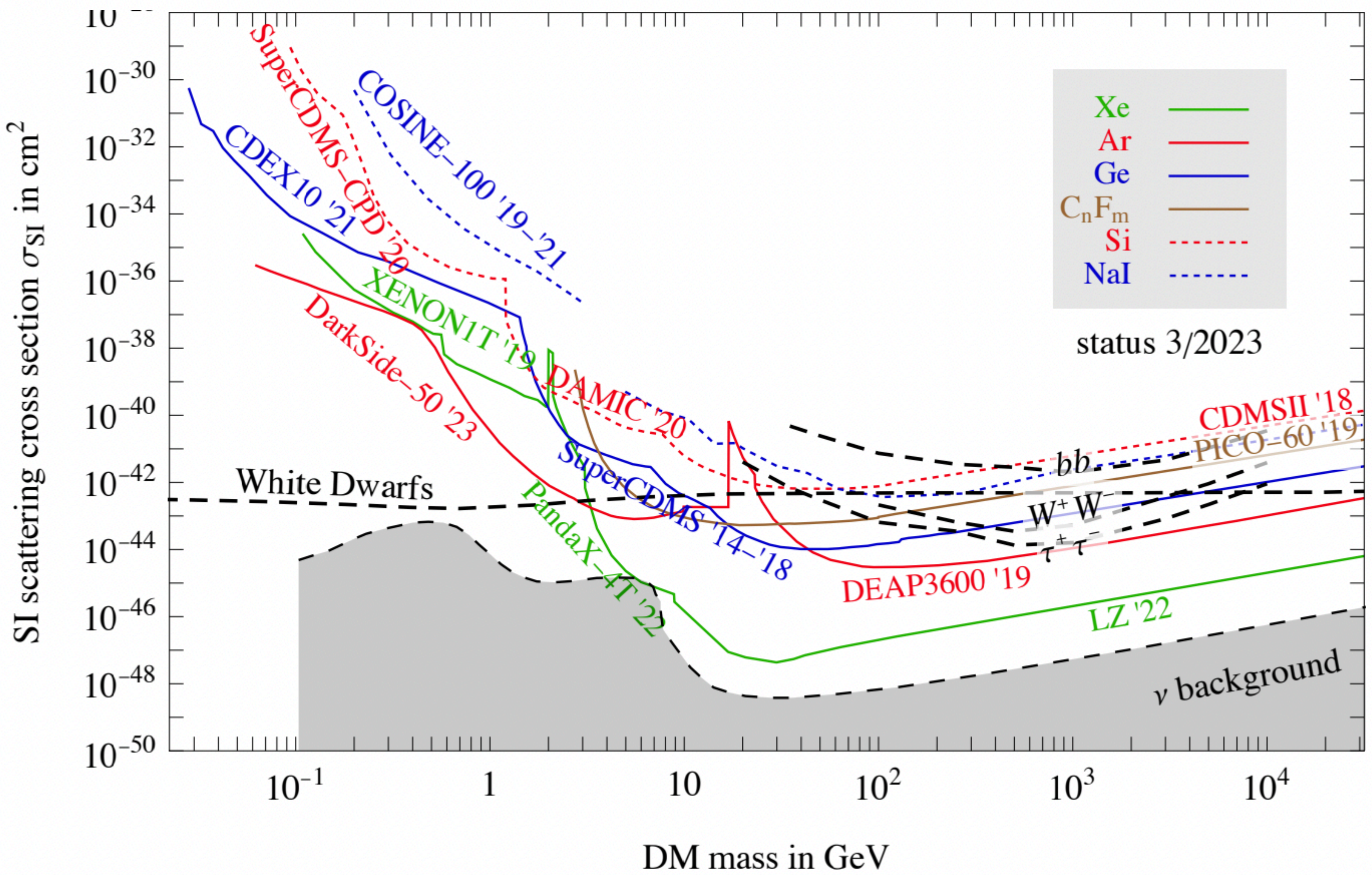

M. Cirelli et. al : 2406.01705

Lighter sectors ??

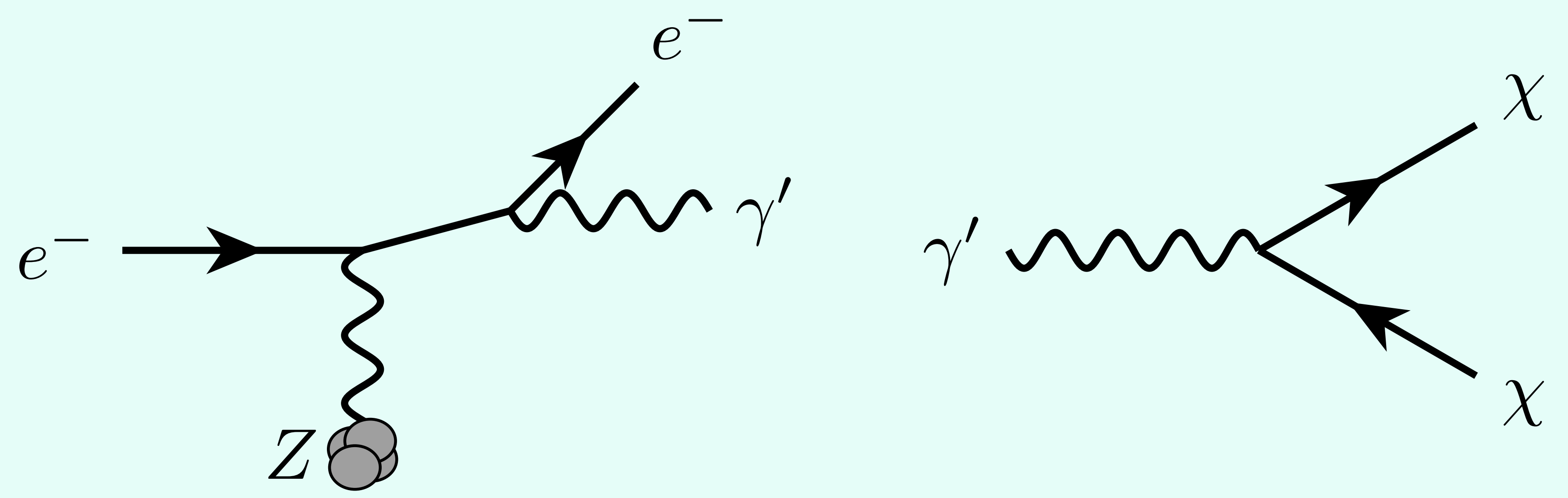

Beam-dumps

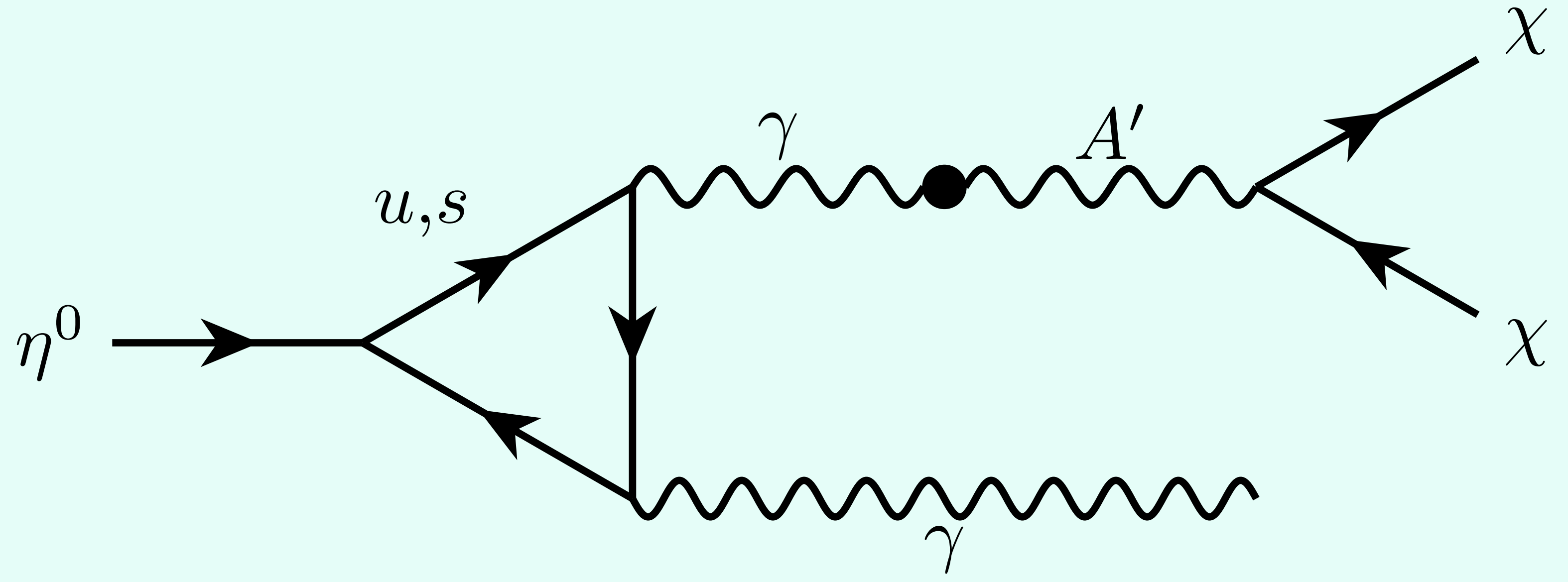

Rare decays of mesons

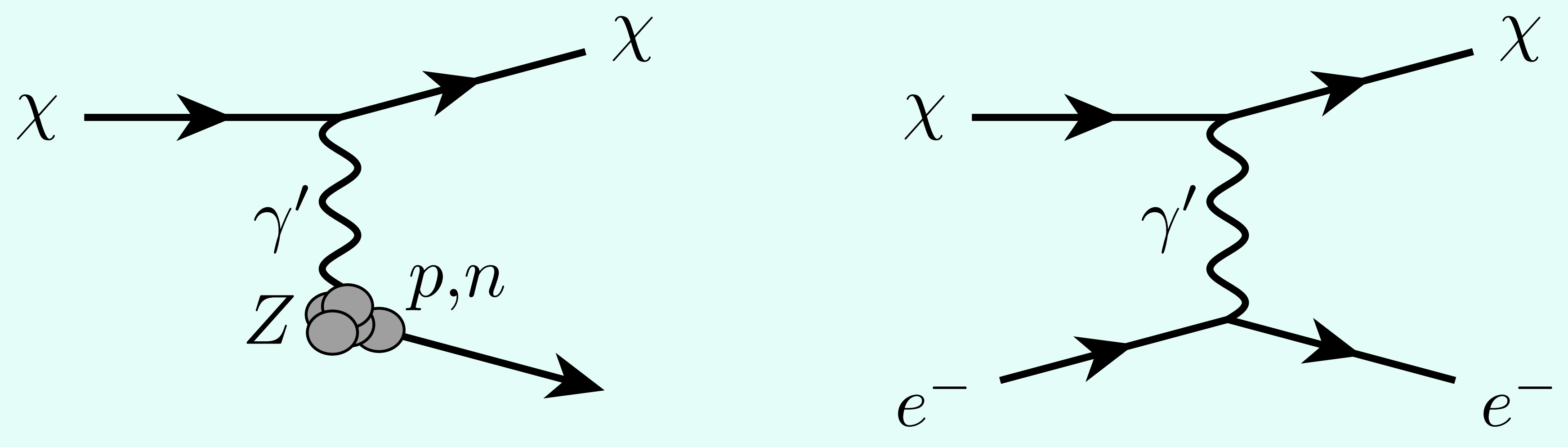

scattering with nuclei/electrons

Lighter sectors ??

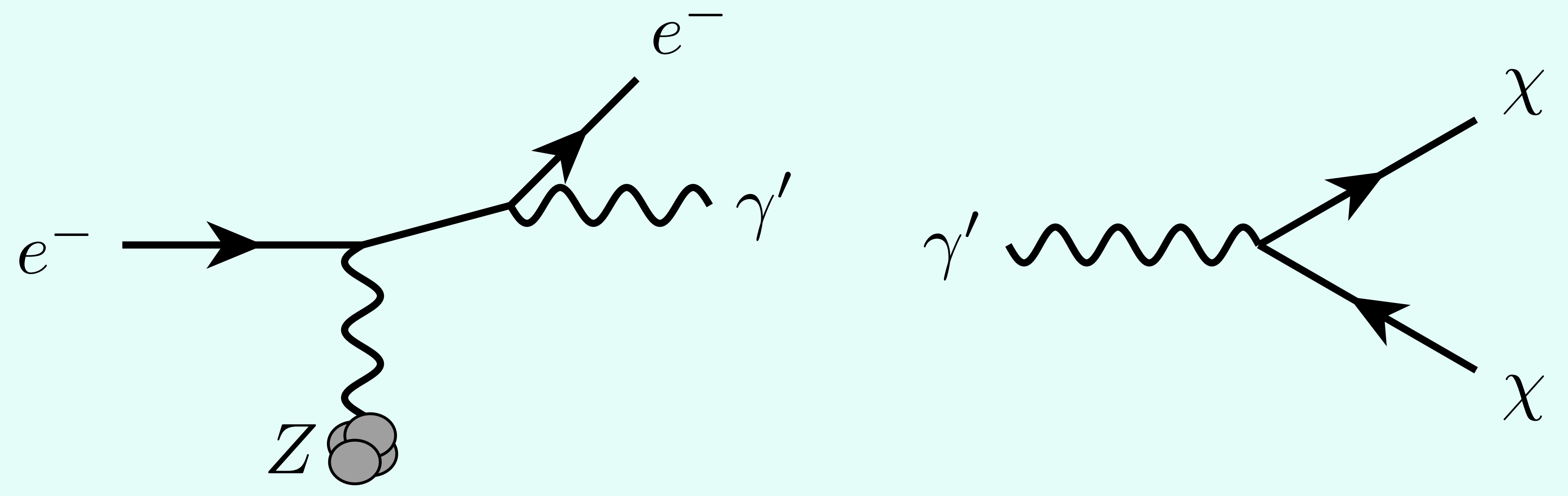

Beam-dumps

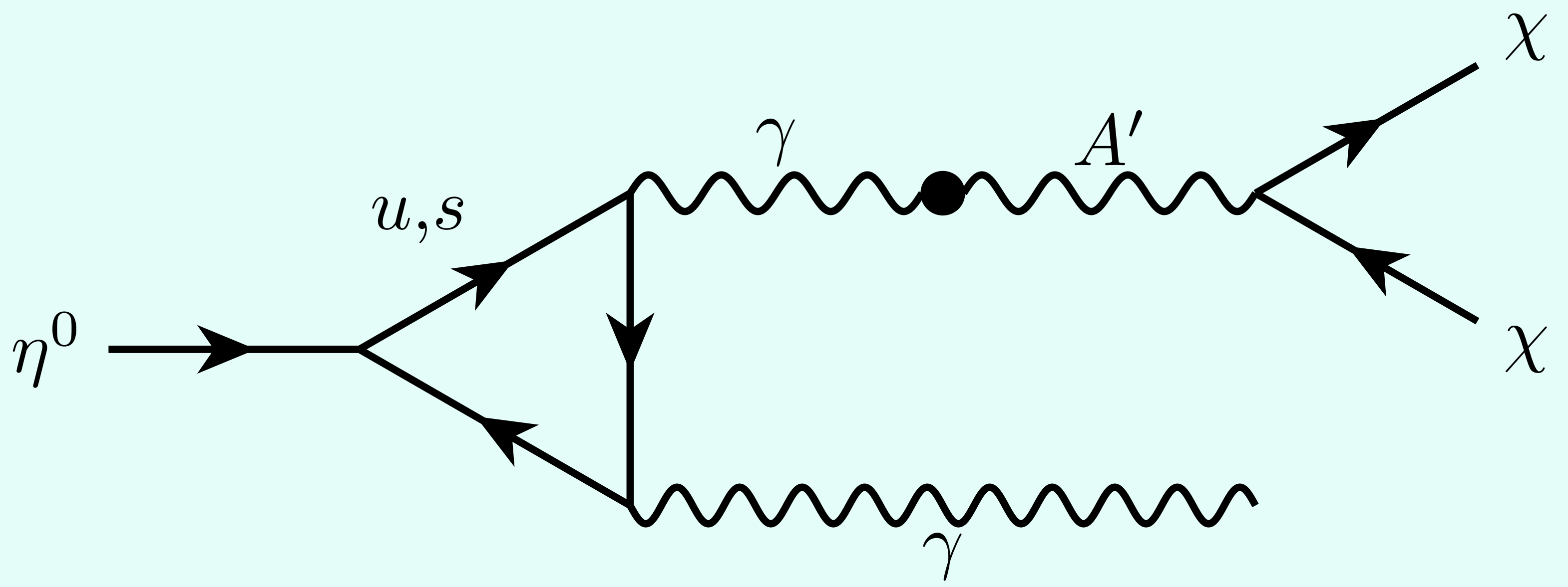

Rare decays of mesons

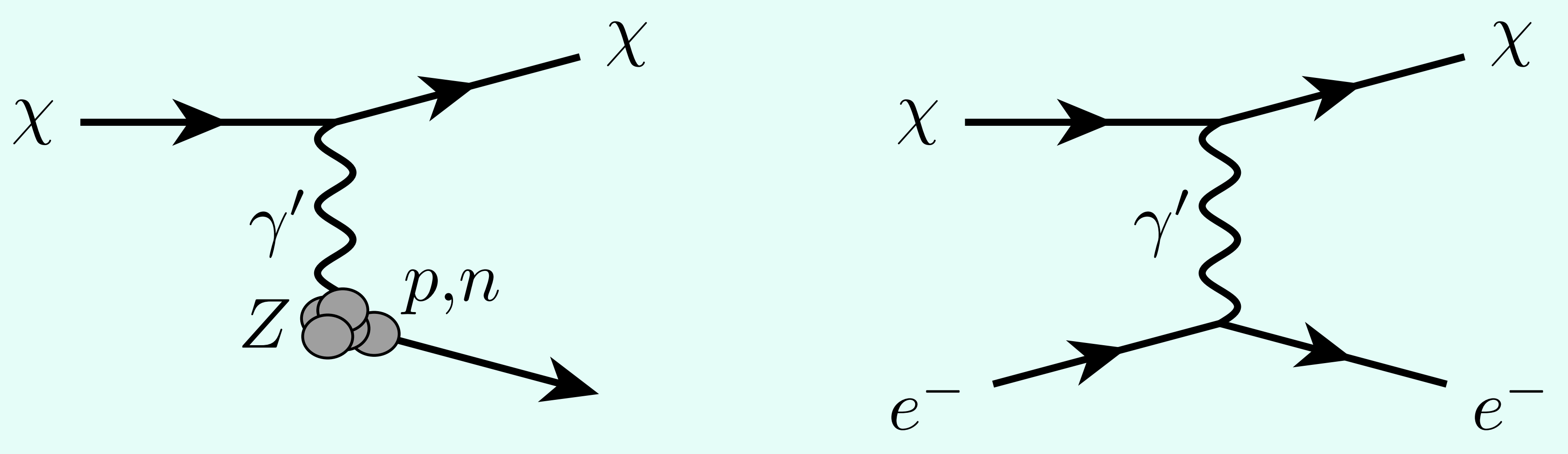

scattering with nuclei/electrons

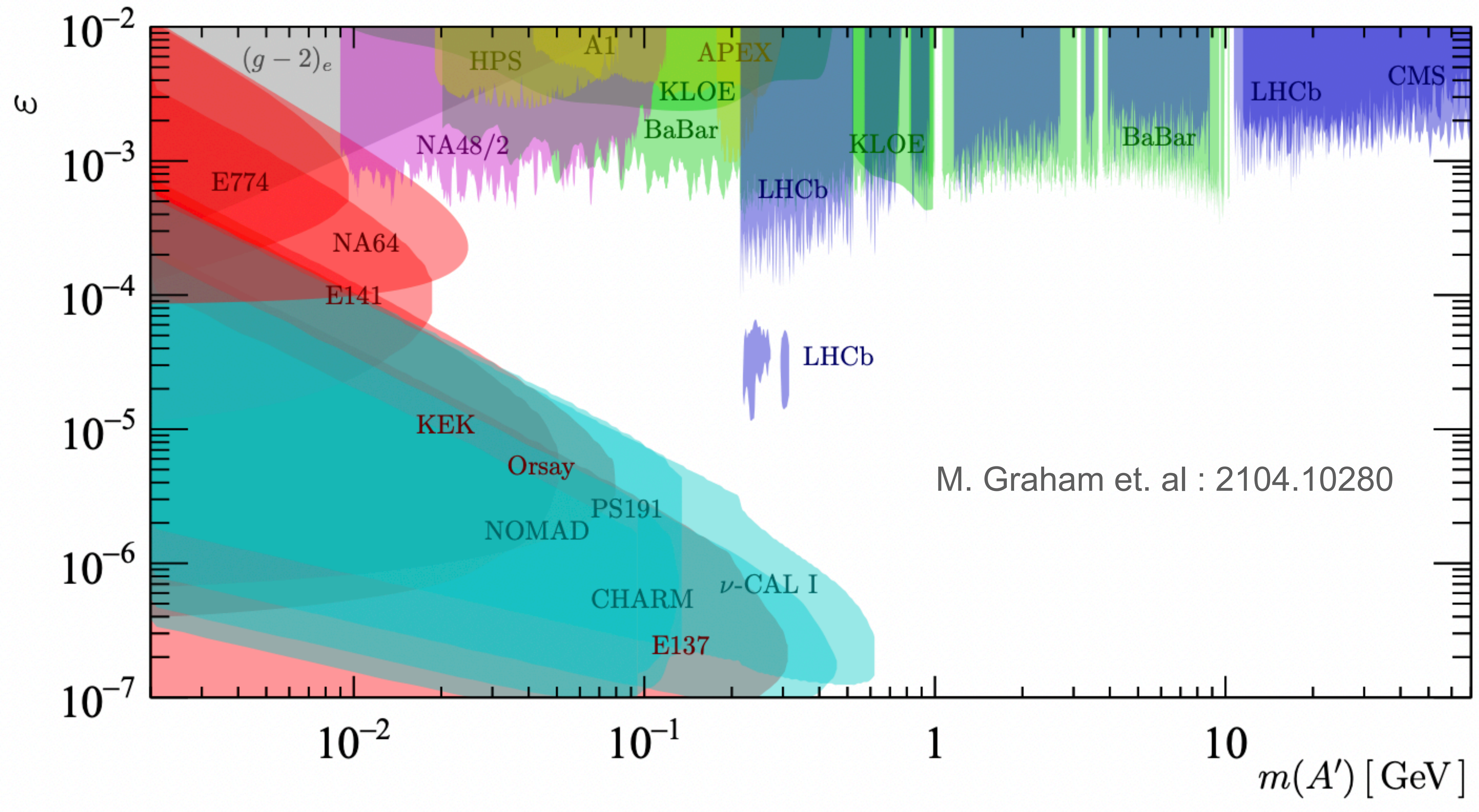

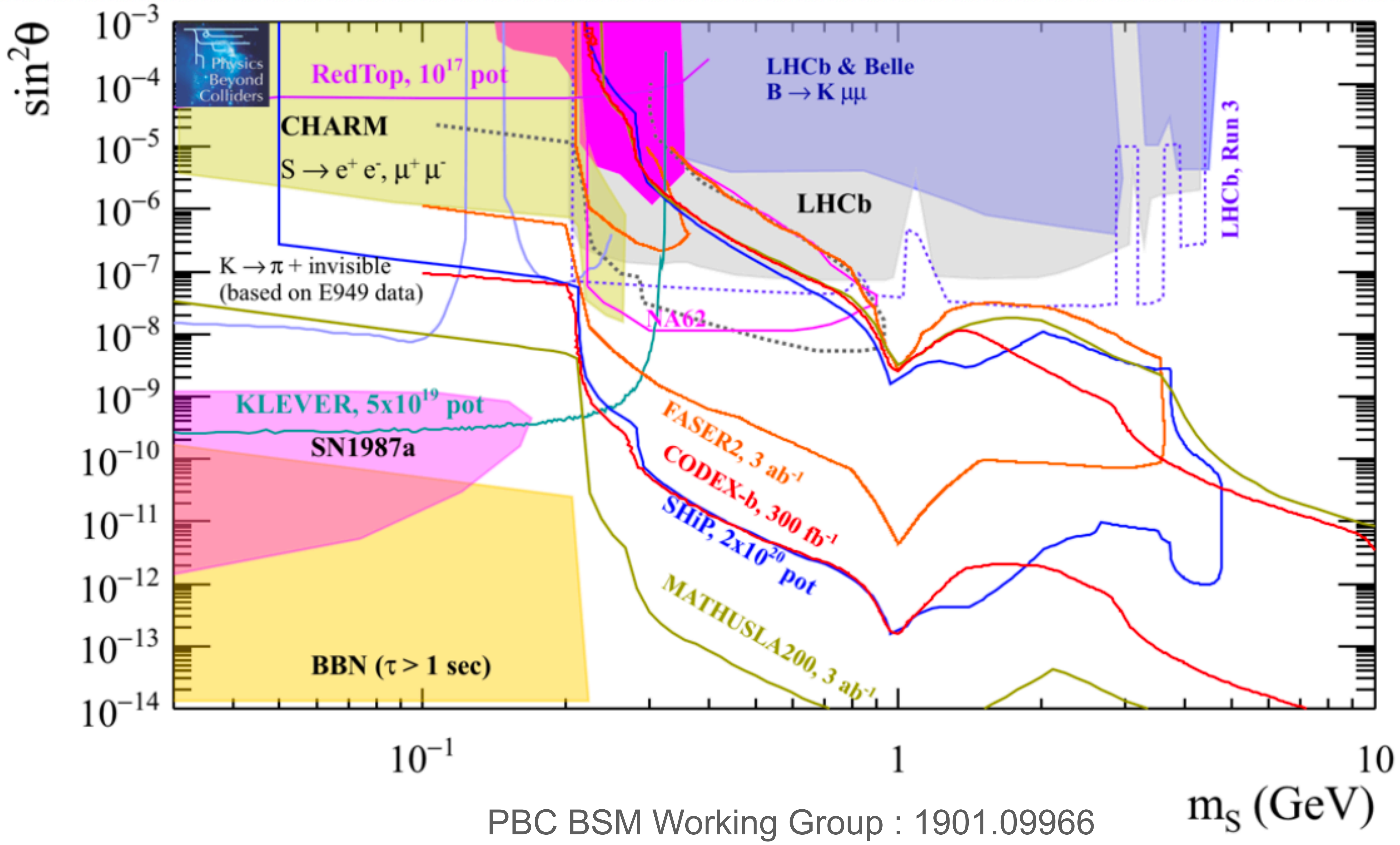

Alternatives ??

Wave-like dark matter

fixed by the halo size, $\lambda \sim \mathcal{O}(\mathrm{kpc})$

classical prescription, $n_\phi \left(\lambda_{\mathrm{coh}}/2\pi\right)^3 >> 1$

- Spin-0 dark matter in the mass range $\approx 10^{-22}$ **eV** $\lesssim m_\phi \lesssim 1$ **eV**
- When these light bosons constitute the majority of the dark matter, the number density of the bosonic field inside galactic halo is large enough so that the dark matter field have a large occupation number, allowing the system to be described effectively as a *classical "wave-like"* field.

$$\boxed{\phi(\vec{x}, t) \approx \underbrace{\frac{\sqrt{2\rho_{\mathrm{DM,local}}}}{m_\phi}}_{\phi_0} \cos\left(m_\phi(t + \vec{\beta}\cdot\vec{x})\right)}$$

$|\vec{\beta}| \approx 10^{-3}$ - dark matter velocity

$\vec{x}$ dependent term amounts to a random phase

We ignore the velocity dispersion term $\propto |\beta|^2$

Ultralight dark matter

Low-mass bosonic particles form a coherently oscillating classical field described by

- Amplitude fixed by dark matter energy density : $\rho_\phi = \frac{1}{2} m_\phi^2 \phi_0^2$ ($\rho_{\mathrm{DM,local}} \approx 0.4\,\mathrm{GeV/cm^3}$)
- The angular frequency determined by the rest mass : $\omega \sim m_\phi$
- Small corrections from the kinetic energy : $\frac{\Delta\omega}{\omega} \sim \frac{\langle v_\phi^2 \rangle}{c^2} \sim 10^{-6}$
- Coherence time is set by the frequency spread : $\tau_{\mathrm{coh}} \sim \frac{2\pi}{\Delta\omega} \sim 10^6\, T_{\mathrm{osc}}$

Ultralight dark matter

- In the early universe, a generic classical bosonic field evolves as $\ddot{\phi} + 3H(t)\dot{\phi} + m_\phi^2\phi = 0$

- When $3H > m_\phi$, the system behaves like an overdamped oscillator - the field remains static.

- Oscillations start when $3H \sim m_\phi$ and the field slowly starts rolling towards its potential minimum

- As the Universe expands, $H < < m_\phi$ and the ultralight field starts oscillating and its energy density scales as $\rho \propto a^{-3}$, like cold dark matter.

$$\Omega_a \sim 0.1 \left[\frac{10^{-17}\,\mathrm{GeV}^{-1}}{f}\right]^2 \left[\frac{m_a}{10^{-22}\,\mathrm{eV}}\right]^{1/2}$$

Misalignment mechanism

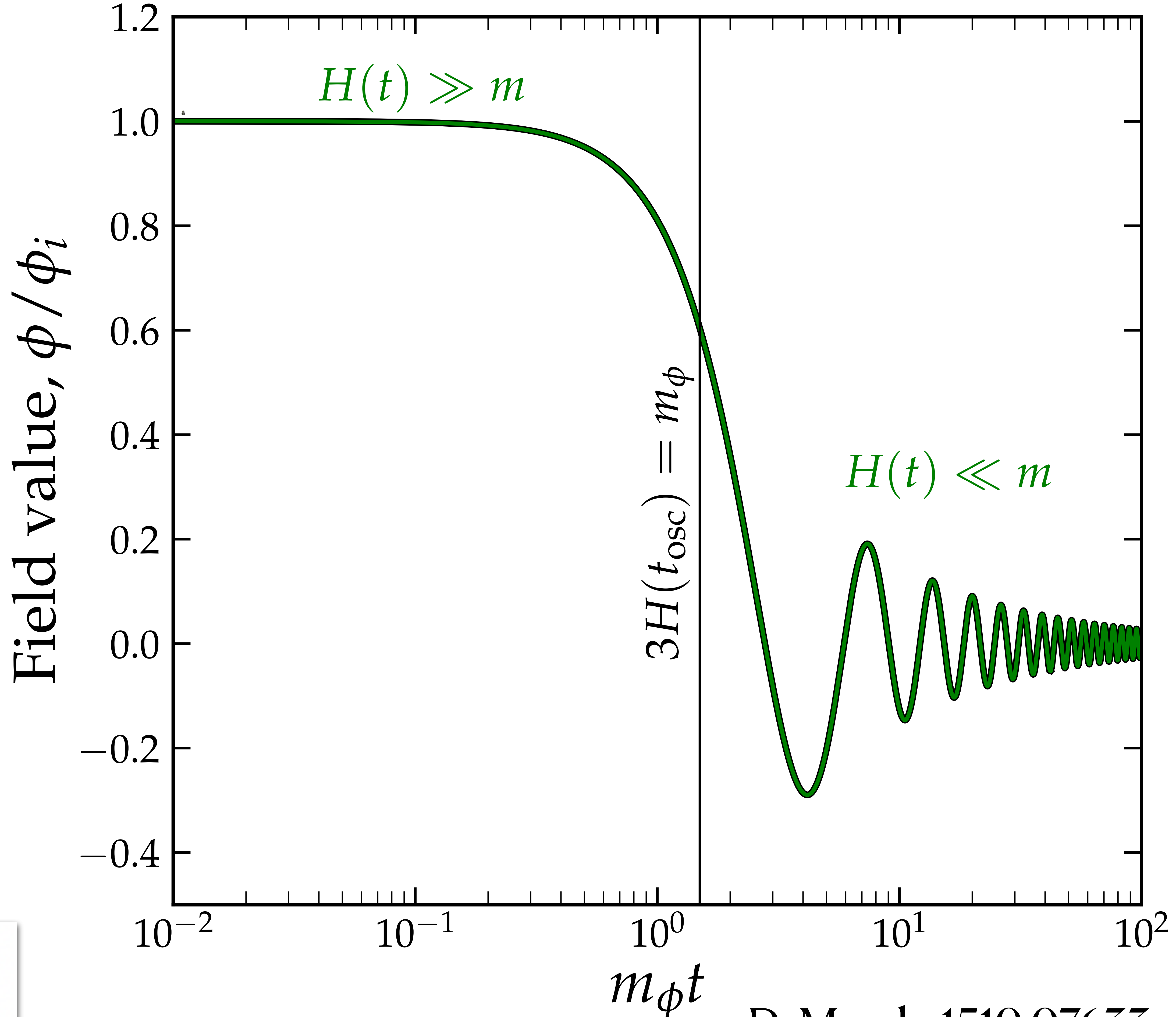

D. Marsh, 1510.07633

C. O'Hare, 2403.17697

Axion-like particle interactions at different scales

- At the UV scale ALPs interact with quarks, gluons and other SM particles

$$\mathscr{L}_{\rm eff}^{D\leq 5}(\mu > \Lambda_{\rm QCD}) \ni \frac{\partial^\mu a}{2f}\, c_{uu}\, \bar{u}\,\gamma_\mu \gamma_5\, u + \frac{\partial^\mu a}{2f}\, c_{dd}\, \bar{d}\,\gamma_\mu \gamma_5\, d + c_{GG}\frac{\alpha_s}{4\pi}\frac{a}{f} G_{\mu\nu}\tilde{G}^{\mu\nu}$$

- These couplings need to be renormalised consistently and matched to a Lagrangian appropriate for low energy processes. Running and matching changes the axion couplings and introduce new couplings that are not present in the UV theory.
- We do the running of the ALP couplings from the UV scale to the electroweak scale by solving the system of RGEs at the weak scale and adding the matching contributions at EW scale. The ALP couplings at the QCD scale are then determined by step-wise running below the EW scale.

ALP low-energy Lagrangian-linear interactions

- At energy scales below Λ_{QCD}, the relevant ALP couplings to photons, nucleons and electrons are written in the leading order of the expansion of the decay constant f_a as

$$\mathscr{L}_{\mathrm{eff}}^{D\leq 5}(\mu \lesssim \Lambda_{\mathrm{QCD}}) = \frac{1}{2}\left(\partial_\mu a\right)(\partial^\mu a) - \frac{m_{a,0}^2}{2}\,a^2 + \frac{\partial^\mu a}{2f}\,c_{ee}\,\bar{e}\,\gamma_\mu\gamma_5\,e + g_{Na}\frac{\partial^\mu a}{2f}\bar{N}\gamma_\mu\gamma_5 \underbrace{N}_{\downarrow\,(p,n)} + c_{\gamma\gamma}^{\mathrm{eff}}\,\frac{\alpha}{4\pi}\,\frac{a}{f}\,F_{\mu\nu}\,\tilde{F}^{\mu\nu}$$

- We assume that all ALP-interactions at the low scale are CP conserving, such that it has no linear, scalar coupling to any Standard Model degrees of freedom.

Origin of quadratic interactions

- At quadratic order in f_a, ALPs have scalar interactions described by the dim-6 operators

$$\mathscr{L}_{\text{eff}}^{D=6}(\mu \lesssim \Lambda_{\text{QCD}}) = \bar{N}\left(C_N(\mu)\mathbb{I} + C_\delta(\mu)\underset{\substack{\big\downarrow \\ \text{diag}(1,-1)}}{\tau}\right)N\frac{a^2}{f^2} + C_E(\mu)\frac{a^2}{f^2}\bar{e}e + C_\gamma(\mu)\frac{a^2}{4f^2}F_{\mu\nu}F^{\mu\nu}$$

- Coupling to gluons at the UV scale induce quadratic couplings to pions below the QCD scale.

- From chiral Lagrangian, one obtains mixing between the ALP and the pion and in the basis where kinetic and mass terms are diagonal one finds upon expanding in a/f:

$$m_{\pi,\text{eff}}^2(a) = m_\pi^2\big(1 + \delta_\pi(a)\big) \longrightarrow \delta_\pi(a) = -\frac{c_{GG}^2}{2}\frac{a^2}{f^2}\left(1 - \frac{\Delta_m^2}{\hat{m}^2}\right) + \mathcal{O}(\tau_a^2)$$

$\hat{m} = (m_u + m_d)/2, \Delta_m = (m_u - m_d)/2, \tau_a = m_a^2/m_\pi^2$

Origin of quadratic interactions

- For the ALP nucleon quadratic coupling, the leading order term is generated by the higher order operator in the chiral Lagrangian and one can write the universal quadratic ALP interaction with nucleons as

$$\mathscr{L} \ni 4c_1 m_\pi^2\, \delta_\pi(a)\bar{N}N + \dots$$

$c_1 = -\,1.26\ \mathrm{GeV}^{-2}$ (Alarcon *et.al,* 1210.4450)

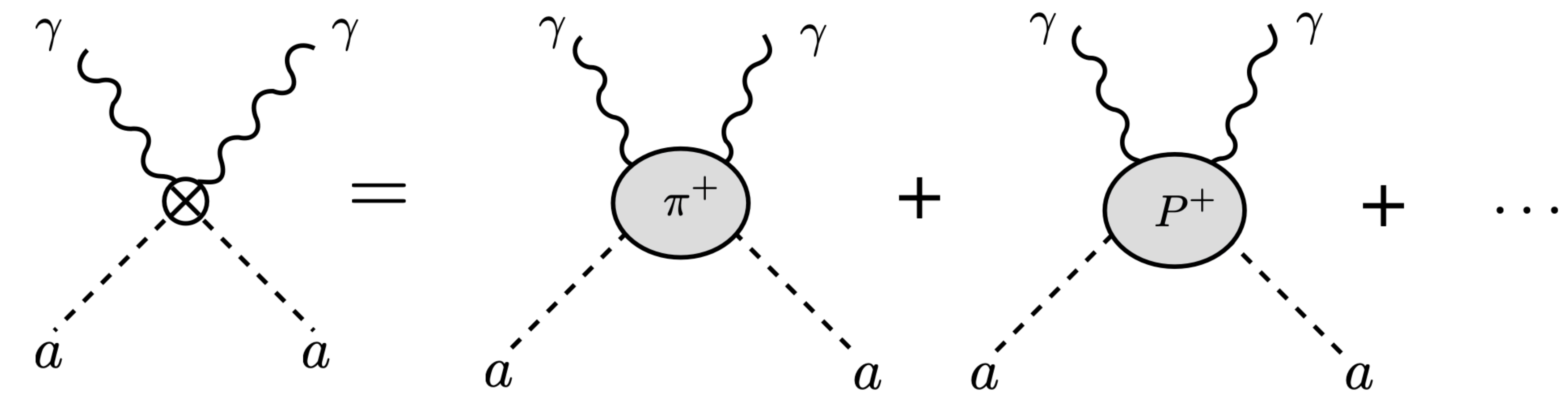

$$C_\gamma(\mu) = \frac{\alpha}{24\pi} c_{GG}^2 \left(-1 + 32c_1 \frac{m_\pi^2}{M_N}\right)\left(1 - \frac{\Delta_m^2}{\hat{m}^2}\right)$$

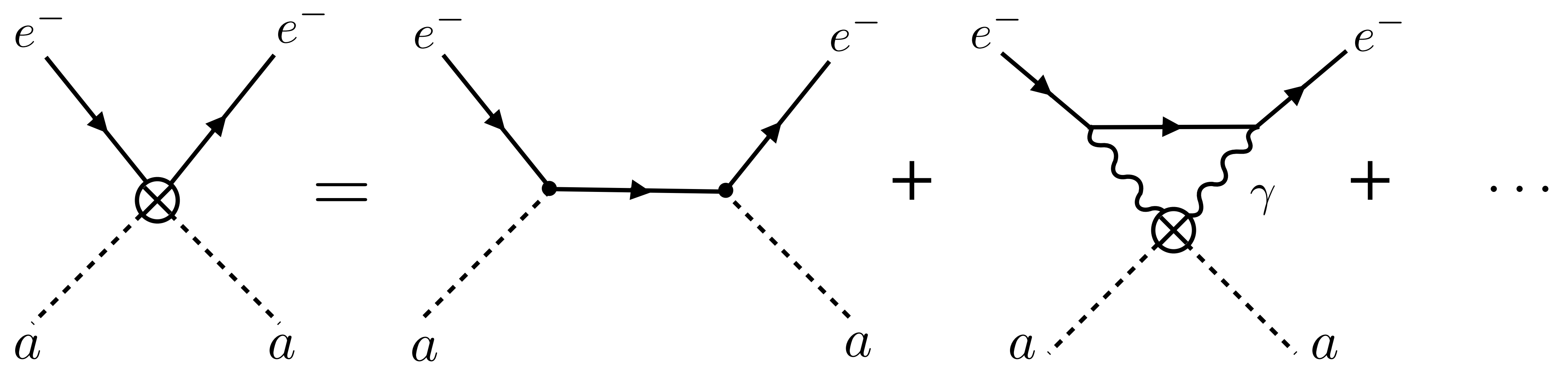

$$C_E = -\,m_e \frac{3\alpha}{4\pi} C_\gamma \ln \frac{m_\pi^2}{m_e^2}$$

More on quadratic interactions

- Quadratic interactions are an unavoidable feature if axion/ALP interacts with gluons at the UV scale.
- The loop-induced quadratic couplings are much more significant than the ones of $\mathcal{O}\left((\partial^\mu a)^2/f_a^4\right)$.
- Quadratic interactions are spin-independent (scalar-like) in nature, so they induce variations of SM couplings and masses, unlike the linear spin-dependent ALP couplings.
- In the oscillating dark matter background, the fundamental constants become field-dependent and their time-dependent variations are measured in the quantum sensors. In axion/ALP dark matter, these probes are achievable uniquely due to the quadratic interactions.

Shifts in fundamental constants

- In the oscillating dark matter background, the low-energy quadratic lagnrangian induces a time-dependent component in the following fundamental constants :

- $\alpha^{\text{eff}}(a) = \Big(1 + \delta_\alpha(a)\Big)\alpha \qquad \text{with} \qquad \delta_\alpha(a) = \frac{1}{12\pi}\left(1 - 32c_1\frac{m_\pi^2}{M_N}\right)\delta_\pi(a)$

- $m_e^{\text{eff}}(a) = m_e\Big(1 + \delta_e(a)\Big) \quad \text{with} \quad \delta_e(a) = \frac{3\alpha}{4\pi}C_\gamma\frac{a^2}{f^2}\ln\frac{m_\pi^2}{m_e^2}$

- $M_N(a) = M_N\Big(1 + \delta_N(a)\Big) \quad \text{with} \quad \delta_N(a) = -4c_1\frac{m_\pi^2}{M_N}\delta_\pi(a)$

Clocks

Basic components

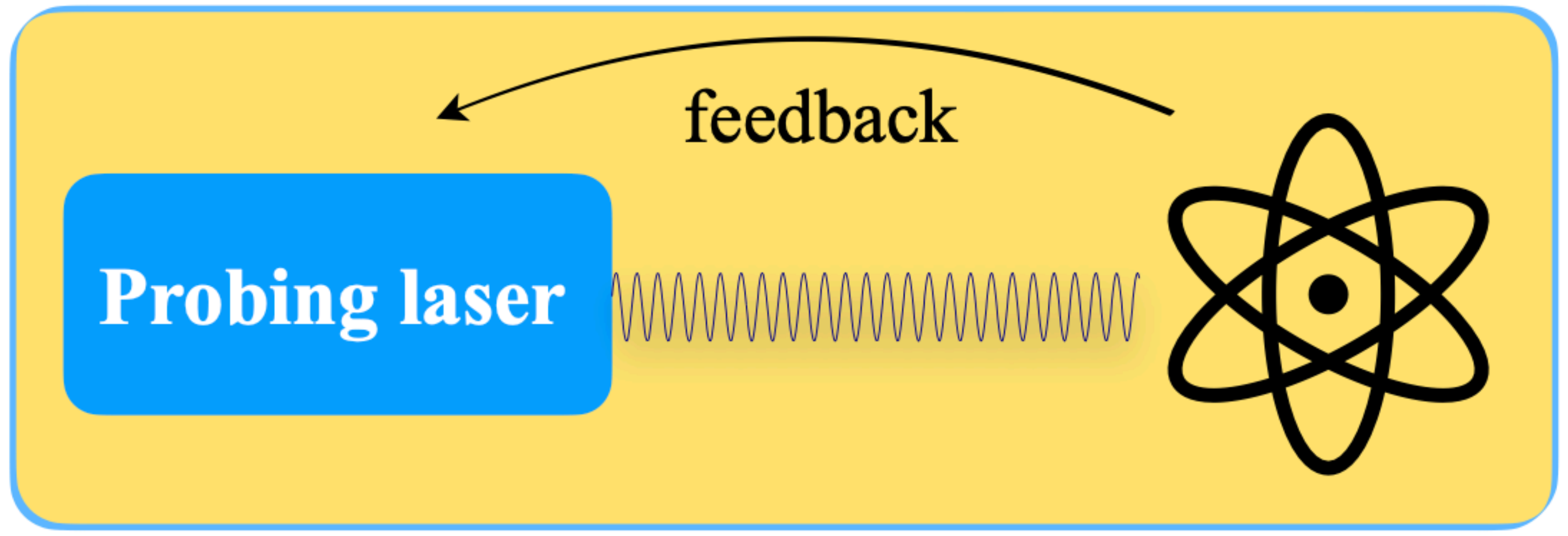

Clock transition

Measured* radiation

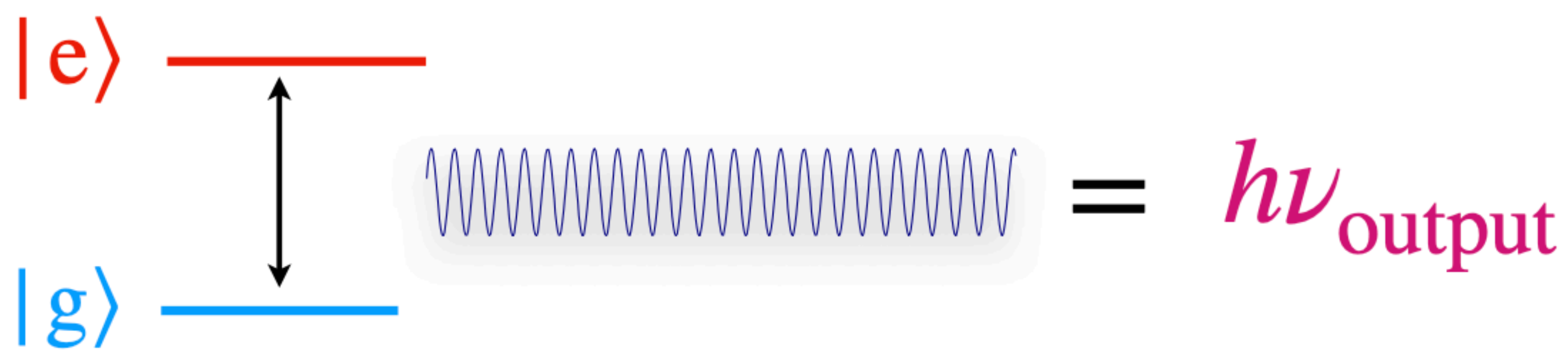

laser/microwave is tuned in resonance with the transition

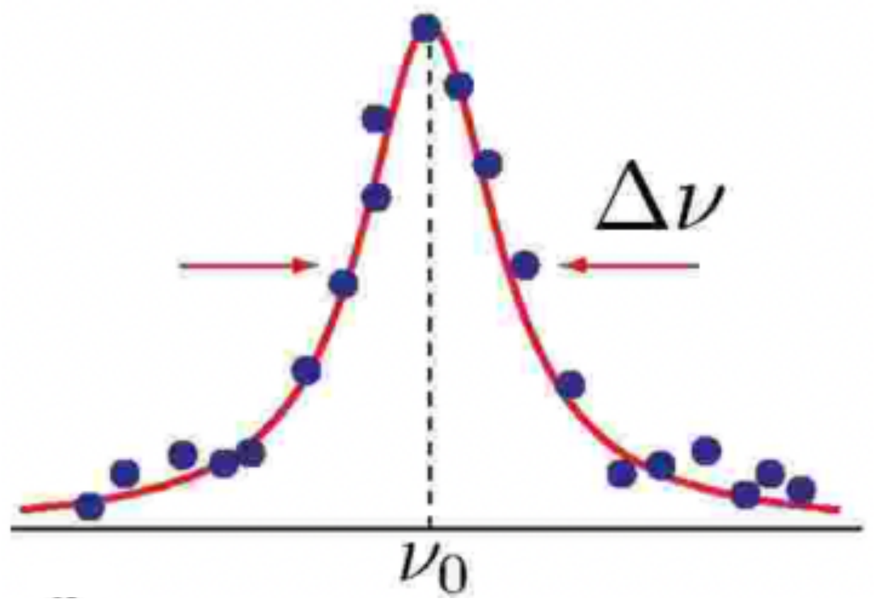

***Cannot measure absolute energies**

$$r_{observable} = \frac{\nu_1}{\nu_2}$$

Different transitions of same system or distinct systems

- Quantum clocks, operate by comparing the frequency ratios of different atomic, vibrational and nuclear transitions.
- Clock frequencies rely on the frequencies of spectral lines in these transitions. Therefore, a fractional change in the spectra brings in a shift in the clock frequency
- Clock searches are naturally broadband, with mass range depending on the total measurement time and specifics of the clock operation protocols

A generic clock prescription

- The frequency ratio of atomic transitions in two different atomic clocks *A* and *B* is parametrised as

Difference in the sensitivity coefficients

$$\nu_{A/B} \propto \alpha^{k_\alpha} \left(\frac{m_e}{m_p}\right)^{k_e} \left(\frac{m_q}{\Lambda_{\mathrm{QCD}}}\right)^{k_q}$$

- To obtain a signal in the clock comparison, the sensitivity coefficients of the two systems must be different

- The observable is the fractional variation in the frequency ratio of A and B :

$$\frac{\delta\nu_{A/B}}{\nu_{A/B}} = k_\alpha \frac{\delta\alpha}{\alpha} + k_e \left(\frac{\delta m_e}{m_e} - \frac{\delta m_p}{m_p} \right) + k_q \left(\frac{\delta m_q}{m_q} - \frac{\delta\Lambda_{\mathrm{QCD}}}{\Lambda_{\mathrm{QCD}}} \right)$$

$$\frac{\delta\nu_{A/B}}{\nu_{A/B}} = k_\alpha\, \delta_\alpha(a) + k_e\, \delta_e(a) - \left(k_e + 2\, k_q\right) \delta_p(a) + k_q\, \delta_\pi(a)$$

- Microwave clocks are based on hyperfine transitions - frequencies of a few GHz. Primarily sensitive to the variations in α and m_e/m_p.
- Optical clocks are based on transitions between different electronic levels - frequencies of $\sim \mathcal{O}(10^{15})$ Hz. Sensitive to variations in α.

In the oscillating dark matter background,

$$\frac{\delta\nu_{A/B}}{\nu_{A/B}} \propto a^2 = \frac{2\rho_{\mathrm{D}M}}{m_a^2} \cos^2 m_a t = \frac{\rho_{\mathrm{D}M}}{m_a^2} \left(1 + \cos 2m_a t\right)$$

$\Rightarrow$ Signal is obtained when Clock frequency $\omega \simeq 2m_a$

Different clock comparisons

Hyperfine frequencies : $\nu \propto \alpha^4 m_e^2 / m_p F_{\rm MW}(\alpha)$

Optical frequencies : $\nu \propto \alpha^2 m_e F_{\rm o}(\alpha)$

clock stability $\propto \nu_0/\Delta\nu$

narrow linewidth gives higher stability

- *Two microwave clocks :* **Rb/Cs** - transitions between different hyperfine levels in the two ground state atoms ^{87}Rb and ^{133}Cs . Sensitive to very low frequencies corresponding to ALP mass $\sim 10^{-20}$ eV and below due to the long time-span of the experiment.
- *Two optical clocks :* **BACON** – $\mathrm{Al}^+/\mathrm{Yb}$, Yb/Sr and $\mathrm{Al}^+/\mathrm{Hg}^+$ frequency comparisons.

– $\mathrm{Yb}^+\ \mathrm{E}_3/\mathrm{E}_2$: comparison between the electric-octupole transition (E_3) and the electric-dipole transition (E_2) of $^{171}\mathrm{Yb}^+$ ion.

– $\mathrm{Yb}^+\ \mathrm{E}_3/\mathrm{Sr}$: frequency ratio between the E_3 transition in $^{171}\mathrm{Yb}^+$ to a transition in the optical lattice clock ^{87}Sr is measured.

- *Optical and microwave clock comparisons :* **Yb/Cs** – all three sensitivity coefficients k_α, k_e and k_q are non-zero, which makes it particularly sensitive to variations in m_e.

Clock-cavity comparison

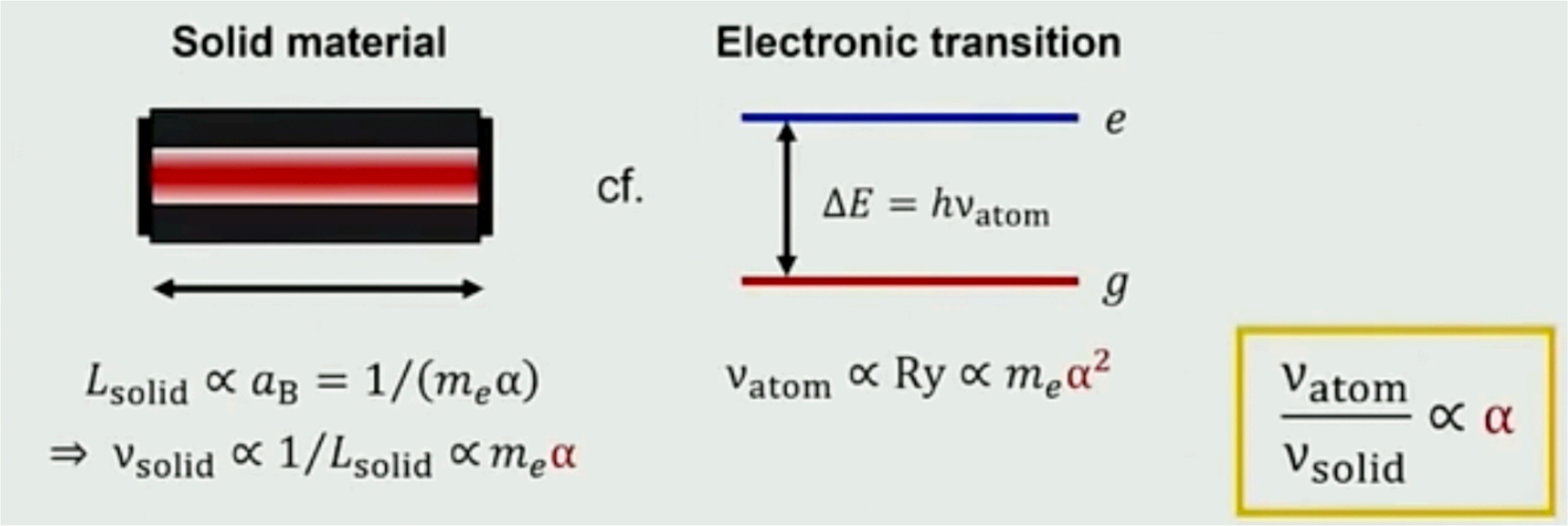

courtesy : Y. Stadnik

- The FC variations in the oscillating DM background induces a change in the length of solid objects such as optical cavities due to variations in Bohr radius.
- The fractional change in the cavity length causes a change in the frequency of the eigenmodes of the cavity, which scales as the inverse of the cavity length.
- The cavity reference frequency, $\nu_c \propto \alpha m_e$ is compared to the atomic transition frequencies in the clocks or other cavities in the optical/microwave domain.

Clock-cavity & cavity-cavity comparisons

- **Sr/Si:** frequency comparison between a Si optical cavity and a ^{87}Sr optical lattice clock. Only sensitive to the variation in the fine-structure constant, due to $\nu_{\text{Sr}} \propto \alpha^{2.06} m_e$. Operates in the optical domain with higher frequency stability and provides the strongest limits in the range $m_a \approx 10^{-17}$ - 2×10^{-16} eV.

Kennedy et. al, Phys. Rev. Lett. 125, 201302 (2020)

- **H/Si:** comparison of the reference frequency of a Si cavity and an H maser. Sensitive to both α and m_e variation because the hyperfine transition frequency of H maser shows a different functional dependence on m_e compared to the cavity frequency - $\nu_H \propto \alpha^4 m_e^2$. Operates in the microwave domain.

- **Cs/D2:** Larger ALP mass is constrained by comparing the measurements of electronic transitions between two states of ^{133}Cs against a laser cavity. Sensitive to FC variations between the acoustic cut-off frequency of the cavity resonator and the frequency of the natural line width of the excited state. Constrains ALPs in the range $m_a \approx 4.6 \times 10^{-11}$ - 10^{-7} eV.

*Antypas et. al, Phys. Rev. Lett. **123**, 141102, Tretiak et. al, Phys. Rev. Lett. 129 (2022)*

How does the parameter space look ?

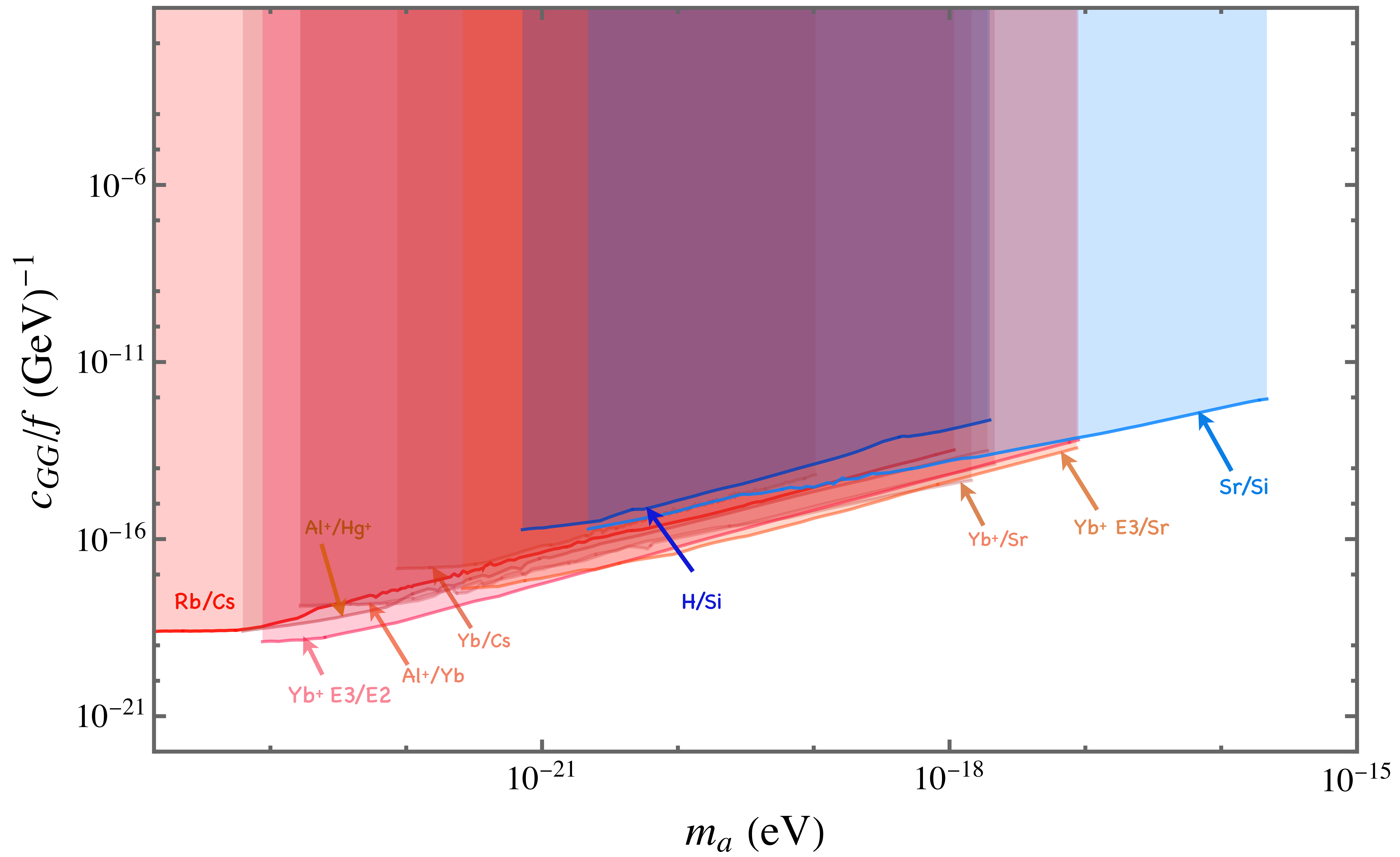

Other experiments probing FC variations??

Optical interferometers

- A two-arm laser interferometer is typically used to detect small changes in the difference of the optical path lengths in the two arms of the interferometer.
- The two arms of an interferometer are practically equal in terms of optical path length. However, the beam splitter can create a geometric asymmetry. The beam-splitter and arm mirrors of an interferometer, if freely suspended, can produce differential optical-path length variations due to changes in the fundamental constants.
- A freely-suspended beam-splitter would experience time-vaying size changes about its centre-of-mass, thus shifting back-and-forth the main reflecting surface that splits and recombines the laser beam would create the phase difference, hence the signal.

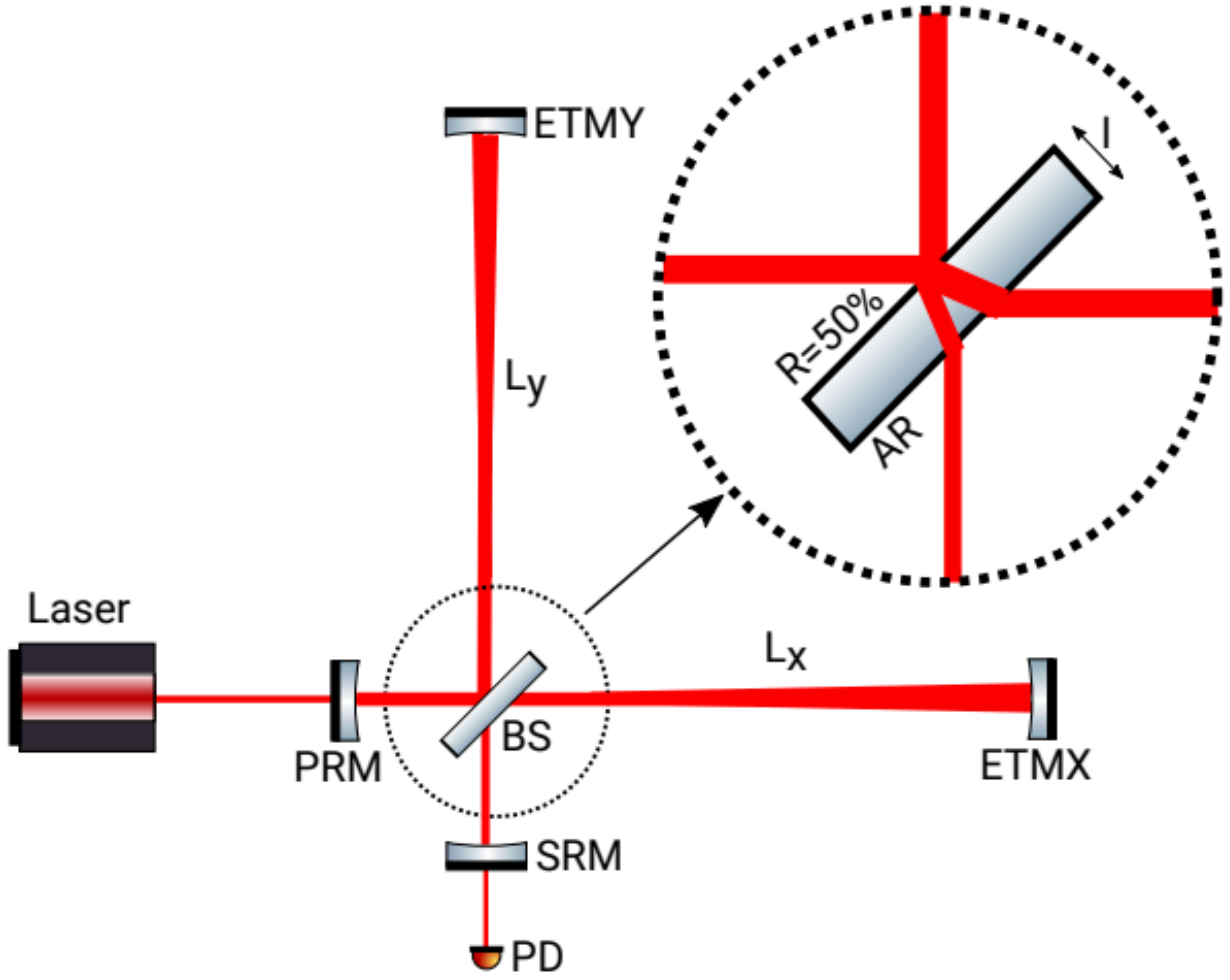

H. Grote1 *et. al*, [arXiv: 1906.06193]

$$\frac{\delta l}{l} = -\left(\frac{\delta\alpha}{\alpha} + \frac{\delta m_e}{m_e}\right) \qquad \delta(L_x - L_y) = \sqrt{2}\left[\left(n - \frac{1}{2}\right)\delta l + l\,\delta n\right] \approx n\,l\,\left[\delta_\alpha(a) + \delta_e(a)\right]$$

$$\frac{\delta n}{n} = -5\times 10^{-3}\left(2\,\frac{\delta\alpha}{\alpha} + \frac{\delta m_e}{m_e}\right)$$

- **GEO-600 –** A modified Michelson's interferometer. The differential strain is derived as a function of frequency to set bounds on the ALP couplings. The entire optimal frequency range of the detector (100 Hz -10 kHz) remains smaller than the fundamental frequency of the longitudinal oscillation mode ~ 37 kHz. Sensitive to the ALP mass range $m_a \approx 10^{-11}$ - 10^{-13} eV.
- **LIGO –** FC oscillations can also be probed with Febry-Perot interferometers like LIGO. The methodology is similar to GEO600 but for LIGO the sensitivity is attenuated by a factor of arm cavity finesse $\sim \mathcal{O}(100)$. There is an additional contribution to $\delta(L_x - L_y)$ from the thickness variation of the mirrors fitted on the two cavity arms. However, this is a subleading effect because $\delta(L_x - L_y) \propto \Delta t \simeq \sim 80\ \mu$m . LIGO-O3 observations set limits in the mass range $m_a \approx 10^{-14}$ - 10^{-11} eV.

Mechanical resonators

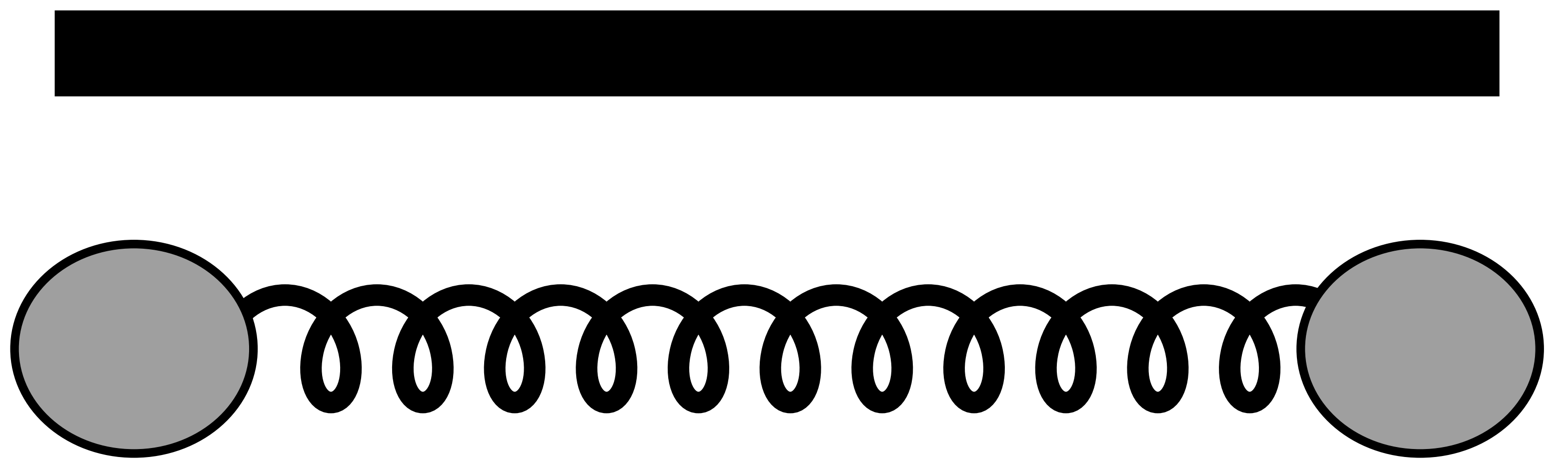

- Similar to optical cavities, mechanical resonators are sensitive to the time variation of the mechanical strain $h(t)$ of solid objects consisting of many atoms, which originates in variations of the atom size caused by FC variations.

$$h(t) = -\left(\delta_\alpha(a) + \delta_e(a)\right)$$

- For quadratic ALP couplings that induce the FC variations above, the strain can be resonantly enhanced if one of the acoustic modes of the elastic body is tuned to twice the ALP Compton frequency.

Mechanical resonators

AURIGA – A cryogenic resonant-mass detector of bar length $\sim \mathcal{O}(\mathrm{m})$. Sensitivity over a narrow bandwidth 850-950 Hz, corresponding to ALP mass window $1.88 - 1.94\ \mathrm{peV}$.

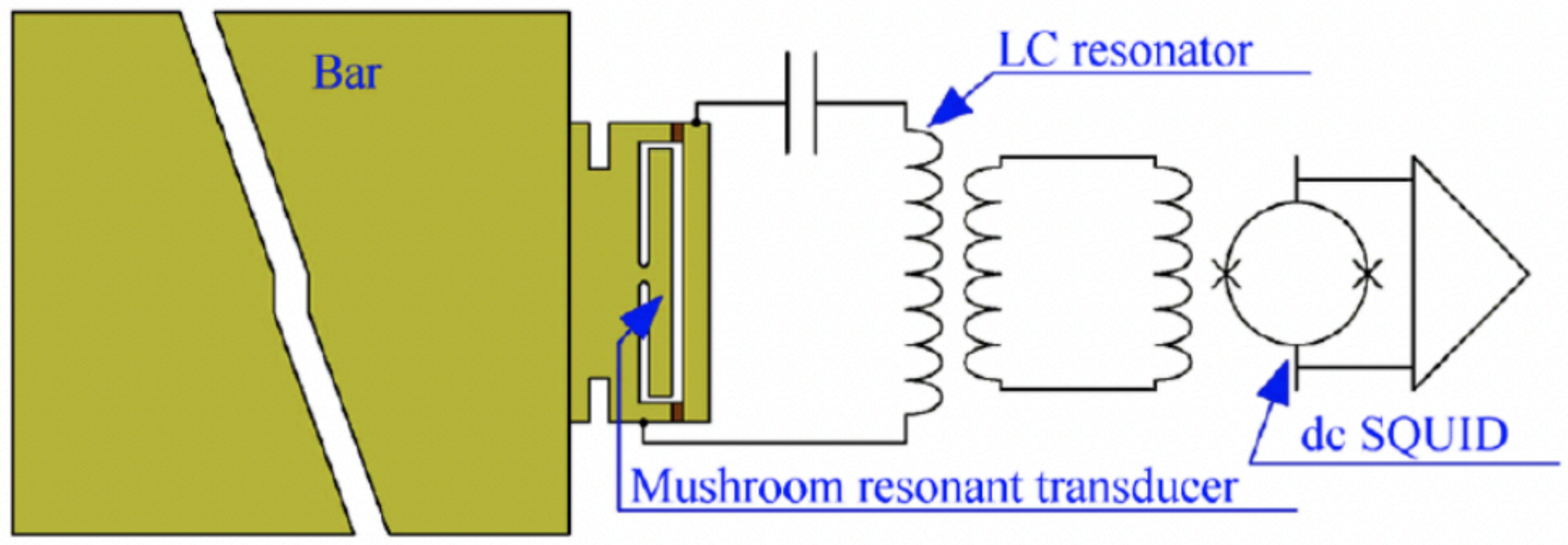

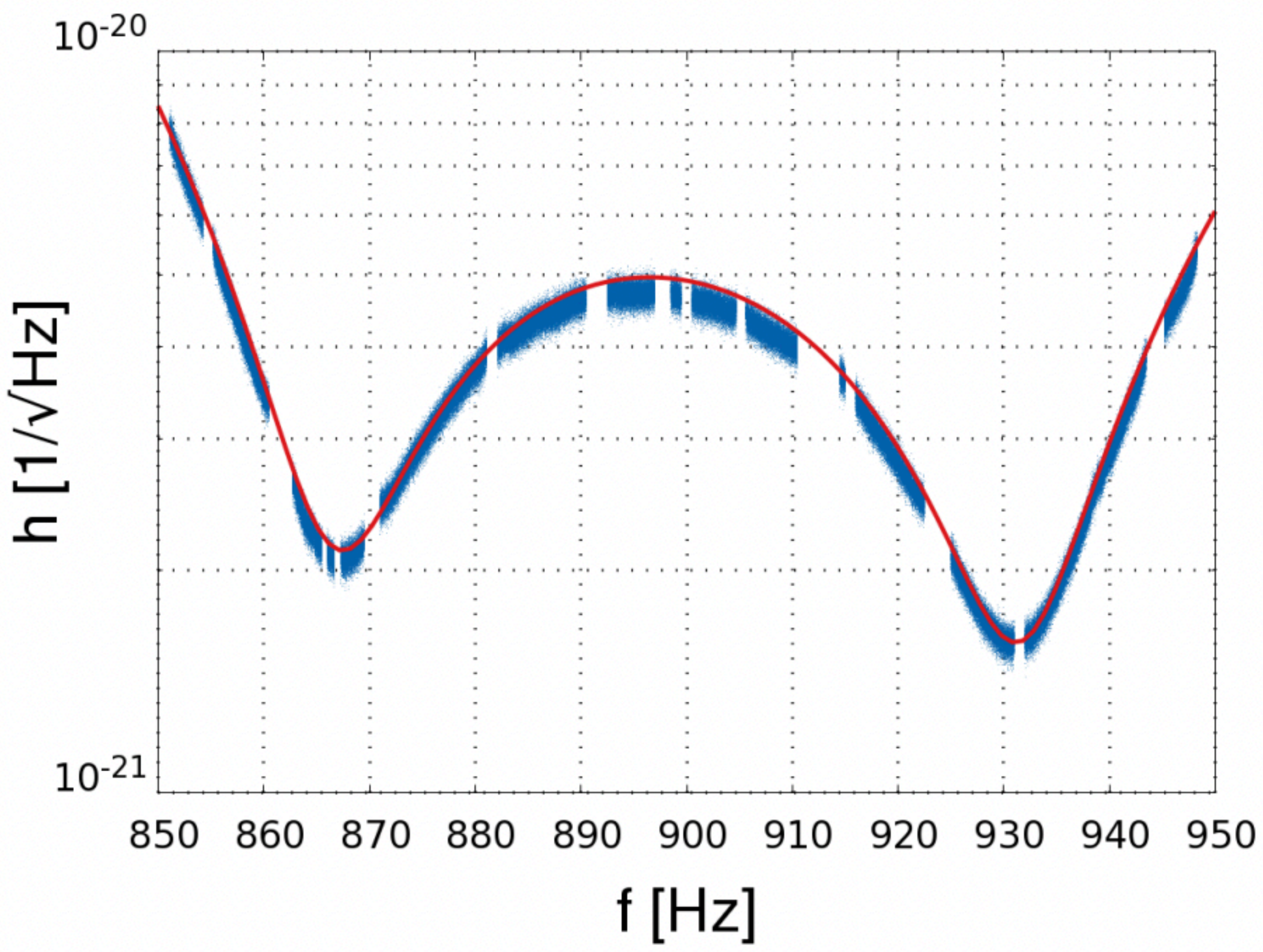

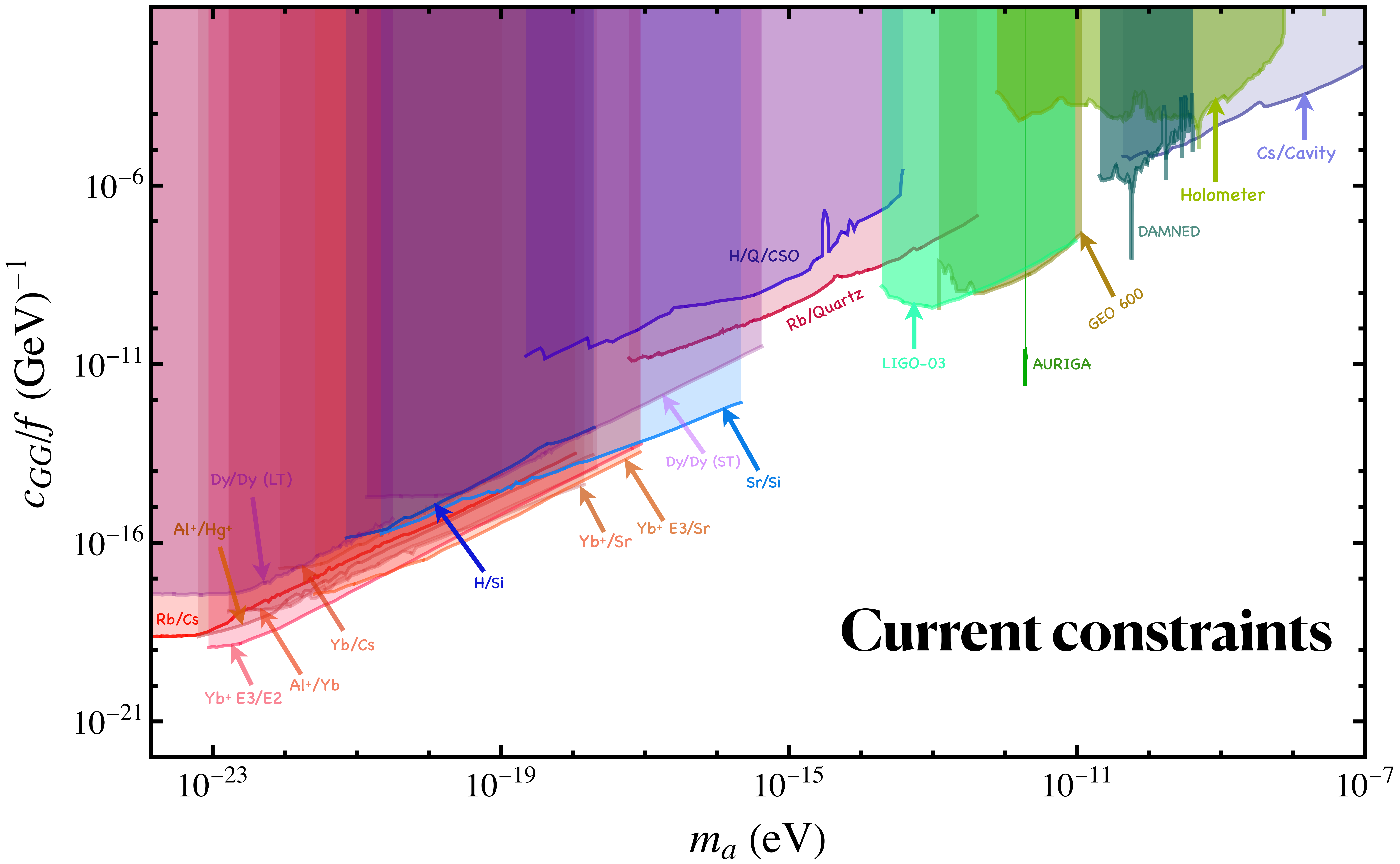

Current constraints
H/Q/CSO
Rb/Quartz
LIGO-O3
AURIGA
GEO 600
DAMNED
Holometer
Cs/Cavity
Dy/Dy (ST)
Sr/Si
Yb+ E3/Sr
Yb+/Sr
H/Si
Dy/Dy (LT)
Al+/Hg+
Rb/Cs
Yb/Cs
Al+/Yb
Yb+ E3/E2
10^{-6}
10^{-11}
10^{-16}
10^{-21}
10^{-23}
10^{-19}
10^{-15}
10^{-11}
10^{-7}
c_{GG}/f (GeV)$^{-1}$
m_a (eV)

Experiments sensitive to linear ALP coupling

Haloscopes

- Haloscopes are microwave cavities tuned to detect the resonant conversion of dark matter ALPs into photons in the presence of a strong static magnetic field
- ALP conversion inside the cavity takes place through " Inverse Primakoff production" which is primarily induced by the linear ALP-photon interaction

$$c_{\gamma\gamma}^{\mathrm{eff}} \frac{\alpha}{4\pi} \frac{a}{f} F_{\mu\nu} \tilde{F}^{\mu\nu} = c_{\gamma\gamma}^{\mathrm{eff}} \frac{\alpha}{\pi} \frac{a}{f} \vec{E} \cdot \vec{B}$$

- In a resonant microwave cavity immersed in a magnetic field, axions interact with the virtual photons of the magnetic field and convert to an oscillating electromagnetic field.
- The ALP conversion maximises if its Compton frequency matches the frequency of a resonant mode of the cavity resonator.

Sikivie Phys. Rev. D 32, 2988 (1985)

Kimball *et. al*, The Search for Ultralight Bosonic Dark Matter

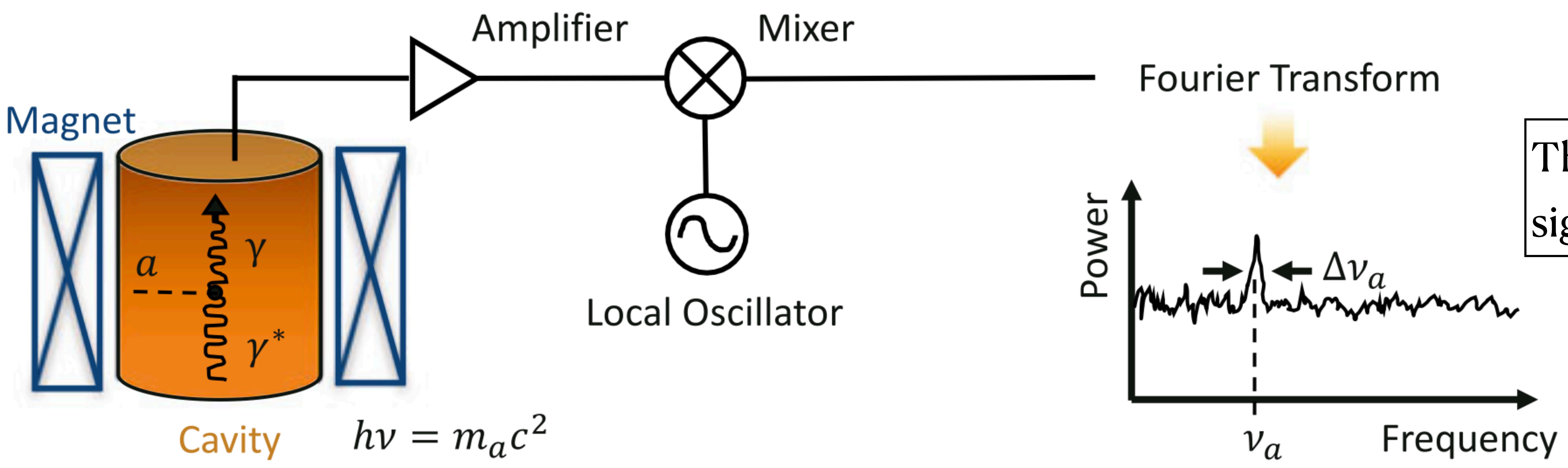

The width of the axion signal $\sim \Delta\nu_a \lesssim 10^{-6}\,\nu_a$

- The resonant conversion condition is that the ALP mass is within the bandwidth of the microwave cavity at its resonance frequency.
- Since the axion mass is unknown, the cavity resonance frequency must be tuned to access a range of axion masses.
- Photons generated from ALP-photon conversion give rise to excess power generation inside the cavity. The frequency dependent signal power extracted on resonance-

$$\boxed{P_{a\to\gamma} = \frac{\alpha^2}{\pi^2}\frac{(c_{\gamma\gamma}^{\text{eff}})^2}{f^2}\frac{\rho_{\text{DM}}}{m_a}B_0^2 VC\min(Q_L, Q_a)}$$

- Cavity haloscopes are designed to probe masses $\sim \mathcal{O}(\mu\mathrm{eV})$.
- Searches for smaller ALP masses would require larger cavities because the volume scales as $V \propto 1/m_a^3$.
- Higher masses require reduced cavity volume which significantly affects the signal power and therefore the scan rate.

Alternatives ??

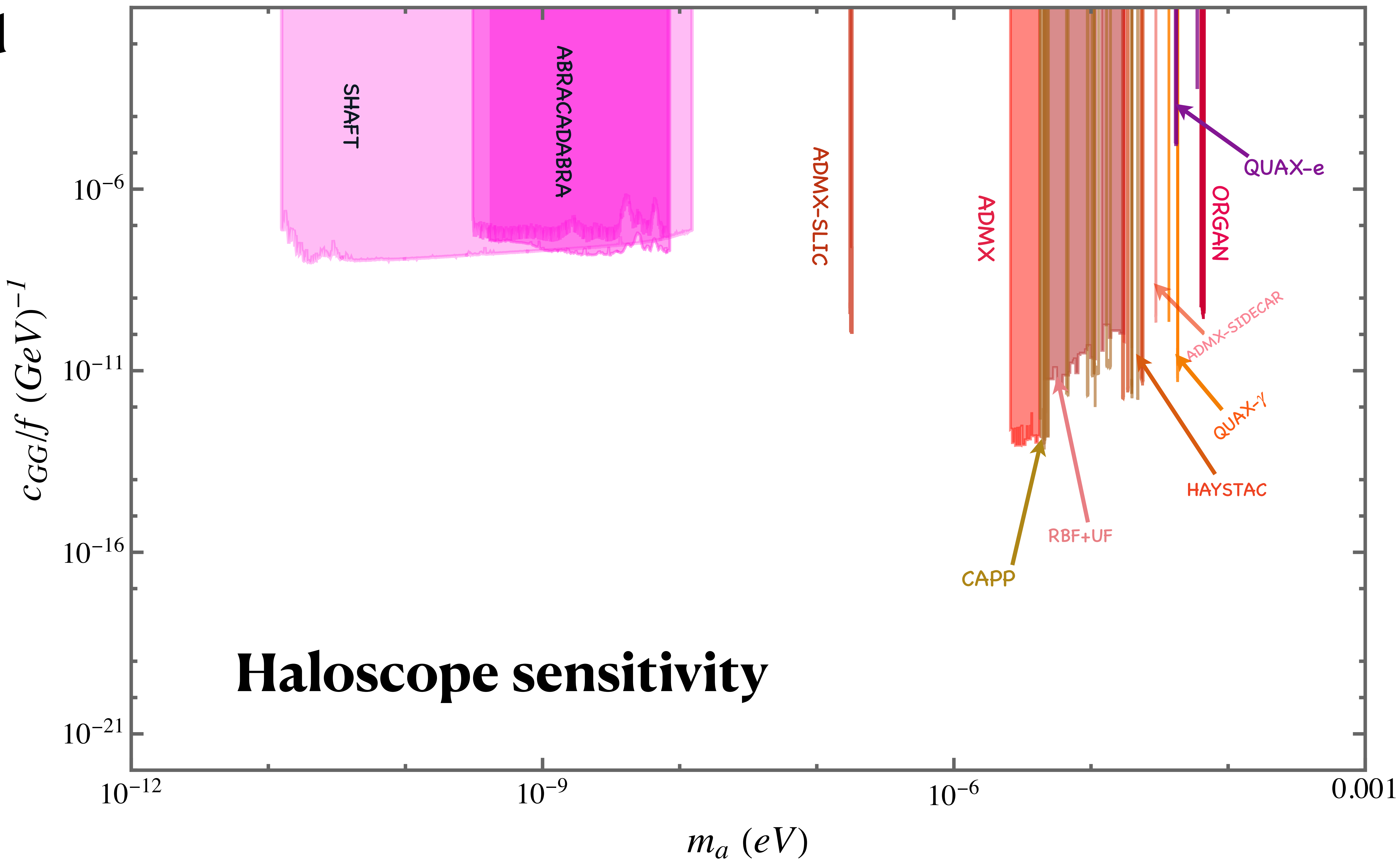

Haloscopes sensitive to quadratic interactions ??

$$\boxed{C_\gamma \frac{a^2}{4f^2} F_{\mu\nu}F^{\mu\nu} = C_\gamma \frac{a^2}{2f^2}(E^2 - B^2)}$$

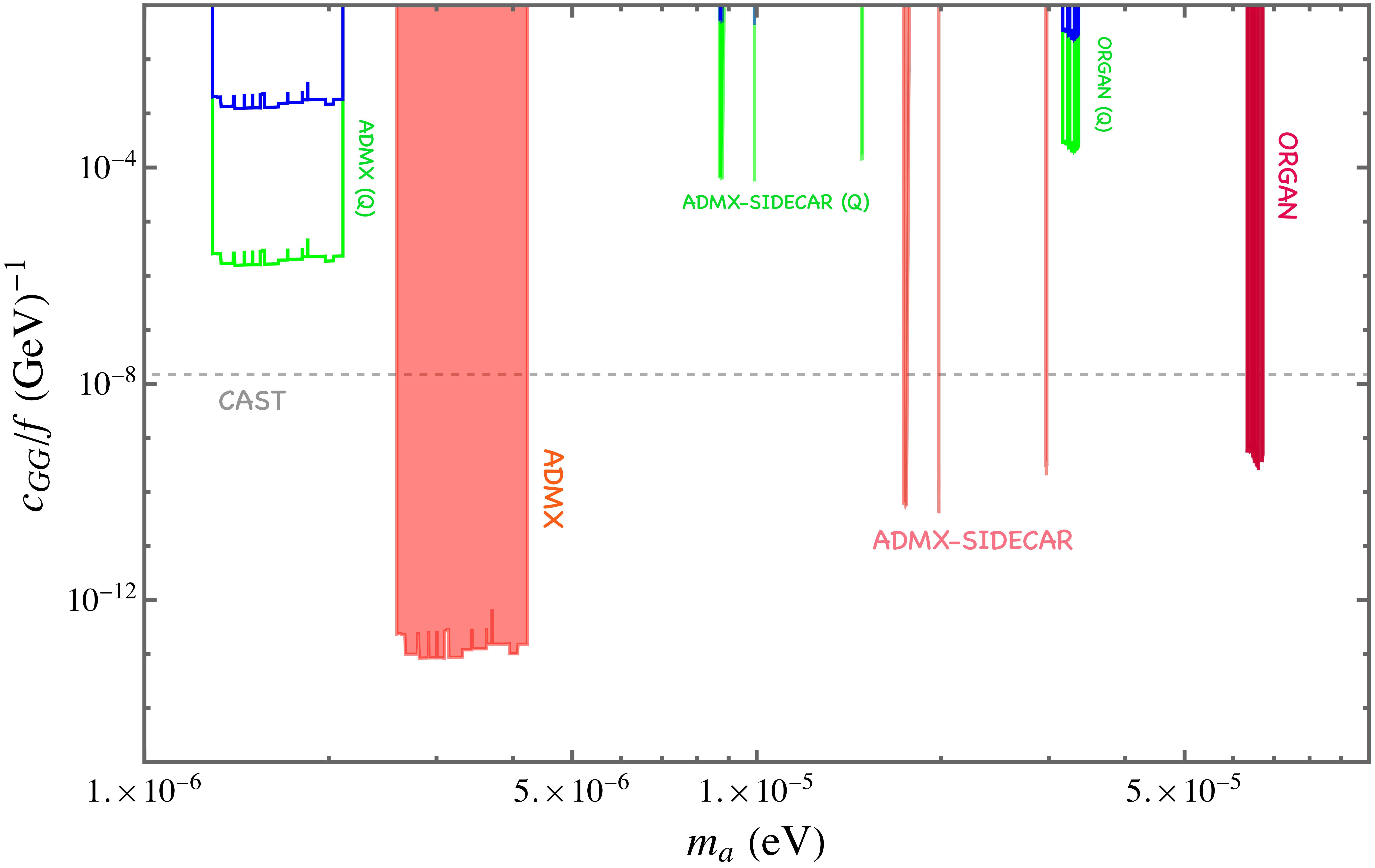

$$P_{aa\to\gamma} \propto \left(\frac{C_\gamma}{f^2}\frac{\rho_{DM}}{m_a}\right)^2 (B_0^2 + E_0^2) V C_\phi \min(Q_L, Q_a)$$

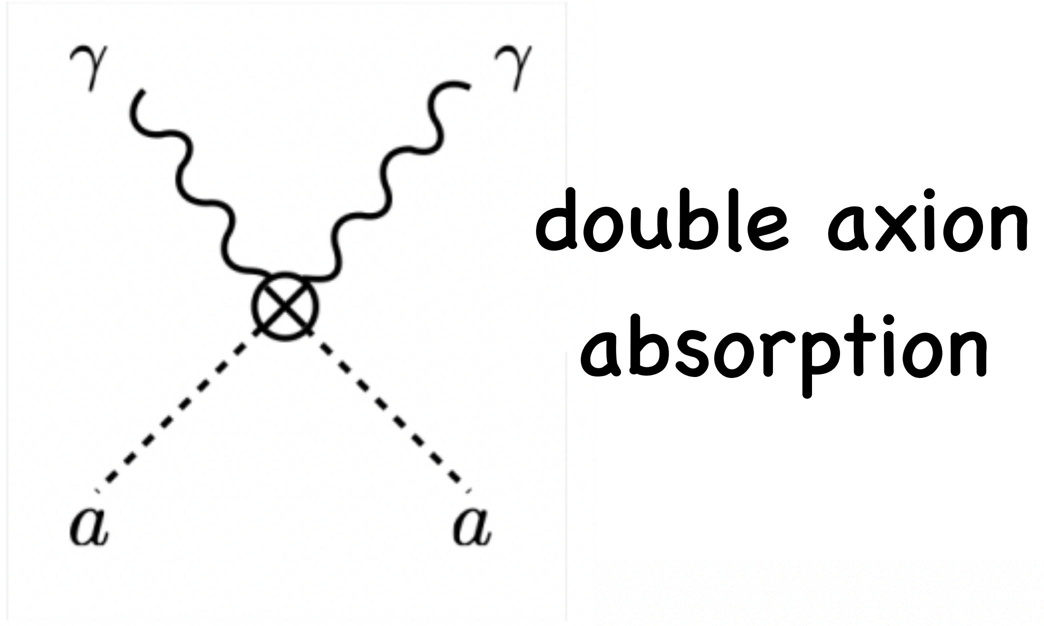

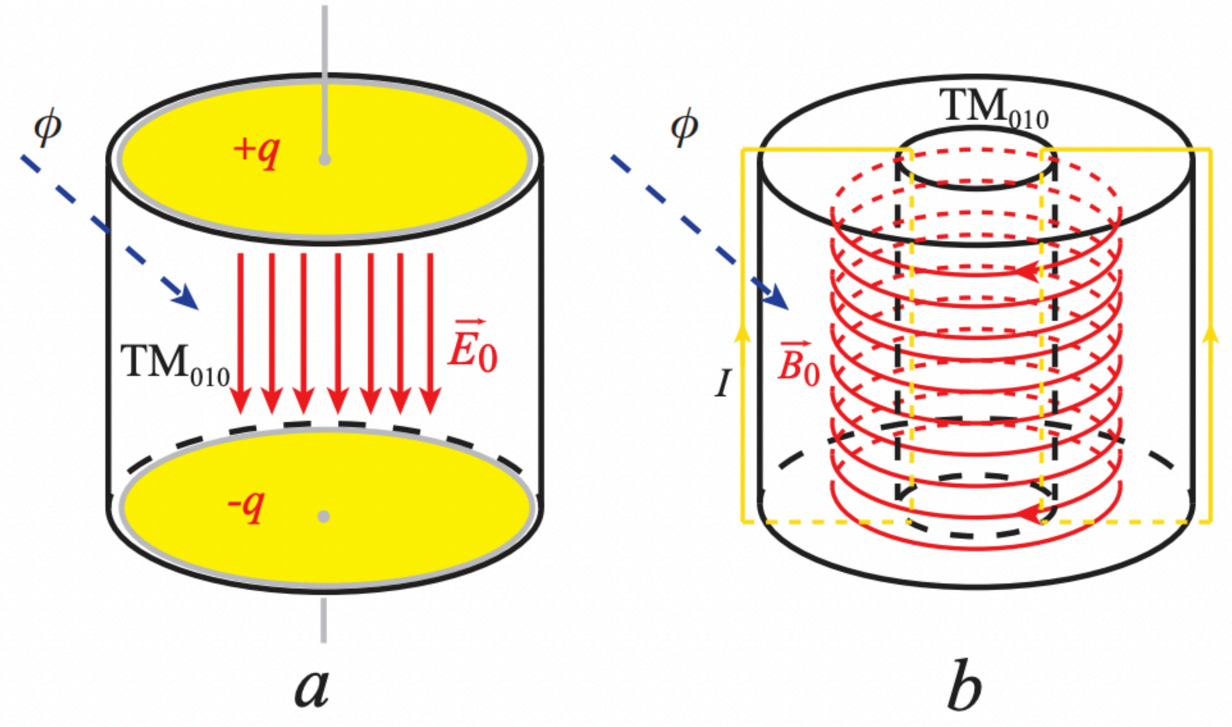

Flambaum et al, Phys. Rev. D 106, 055037, 2022

quadratic interactions allow to extend the parameter space !!

Upcoming facilities

Nuclear clock - ^{229}Th

Seiferle et al., Nature 573, 243 (2019)
T. Sikorsky et al., Phys. Rev. Lett. 125, 142503 (2020)
Caputo et. al, arXiv 2407.17526

Th-229 has an exceptionally low-energy excited isomer state with an excitation energy of a few eV, making it the only nuclear transition accessible to lasers and precision spectroscopy.

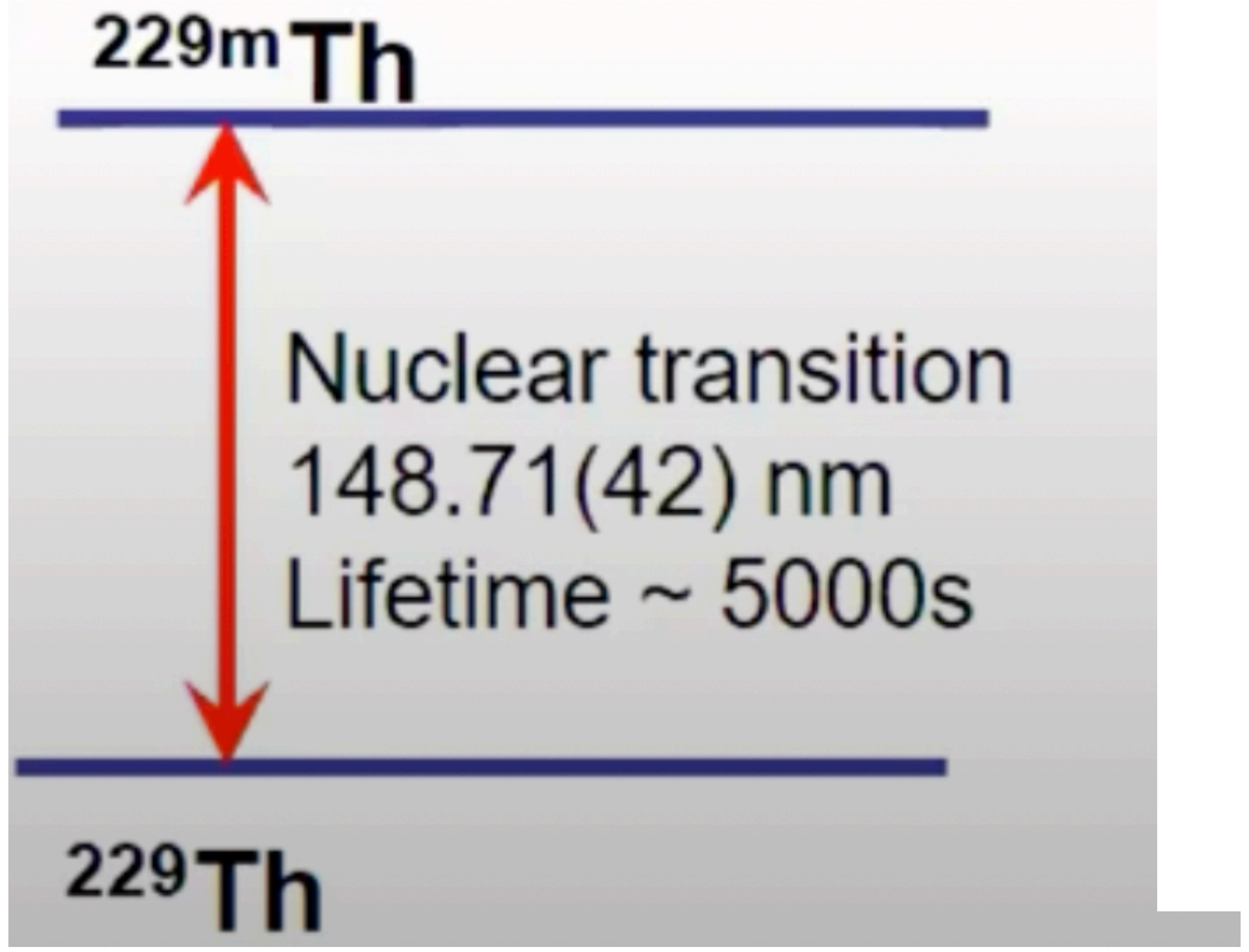

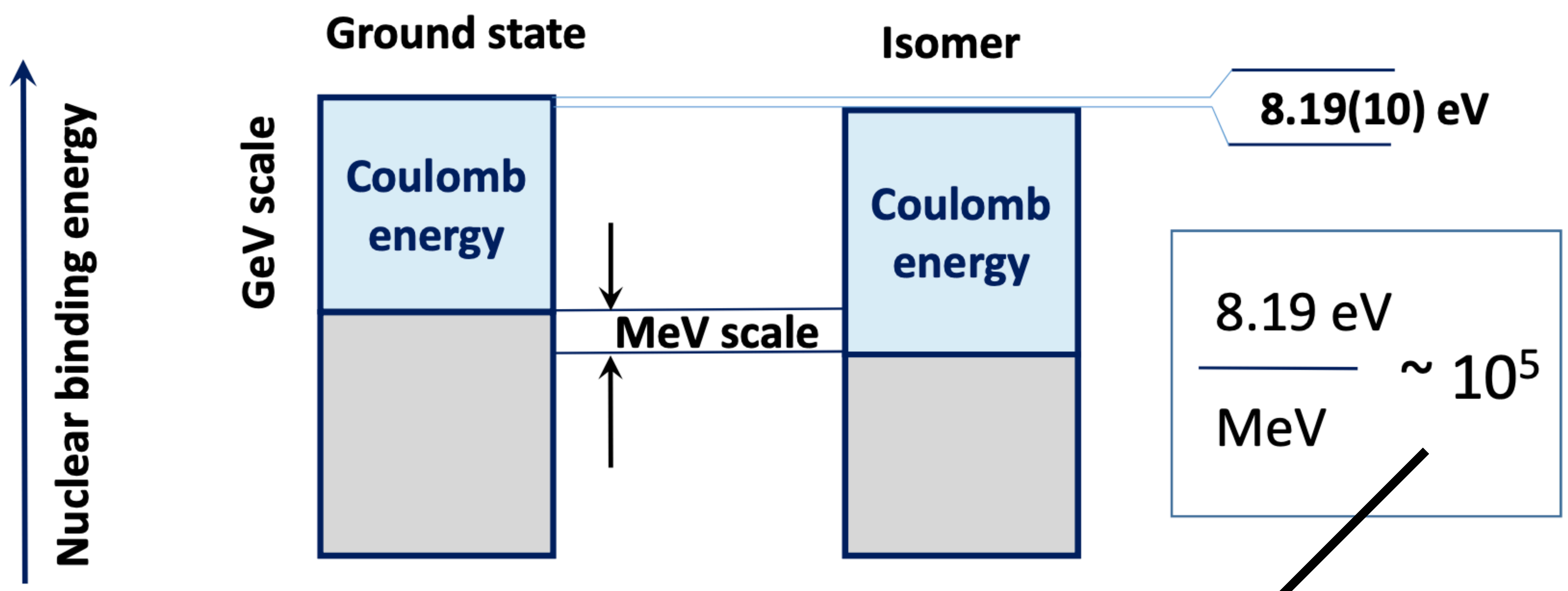

courtesy : M. Safronova

Unprecedented sensitivity - Corresponds to sensitivity coefficients $k_\alpha, k_q \sim \mathcal{O}(10^4 - 10^5)$

Atom interferometers

- Atomic interferometers measure the phase shift between split atomic wave packets and detect a dark matter-induced signal phase when the period of atomic transition oscillation matches the total duration of the interferometric sequence.
- The FC oscillations generate an oscillatory component in the electronic transition frequency, which is $\omega_A \propto m_e \alpha^{2+\xi}$.

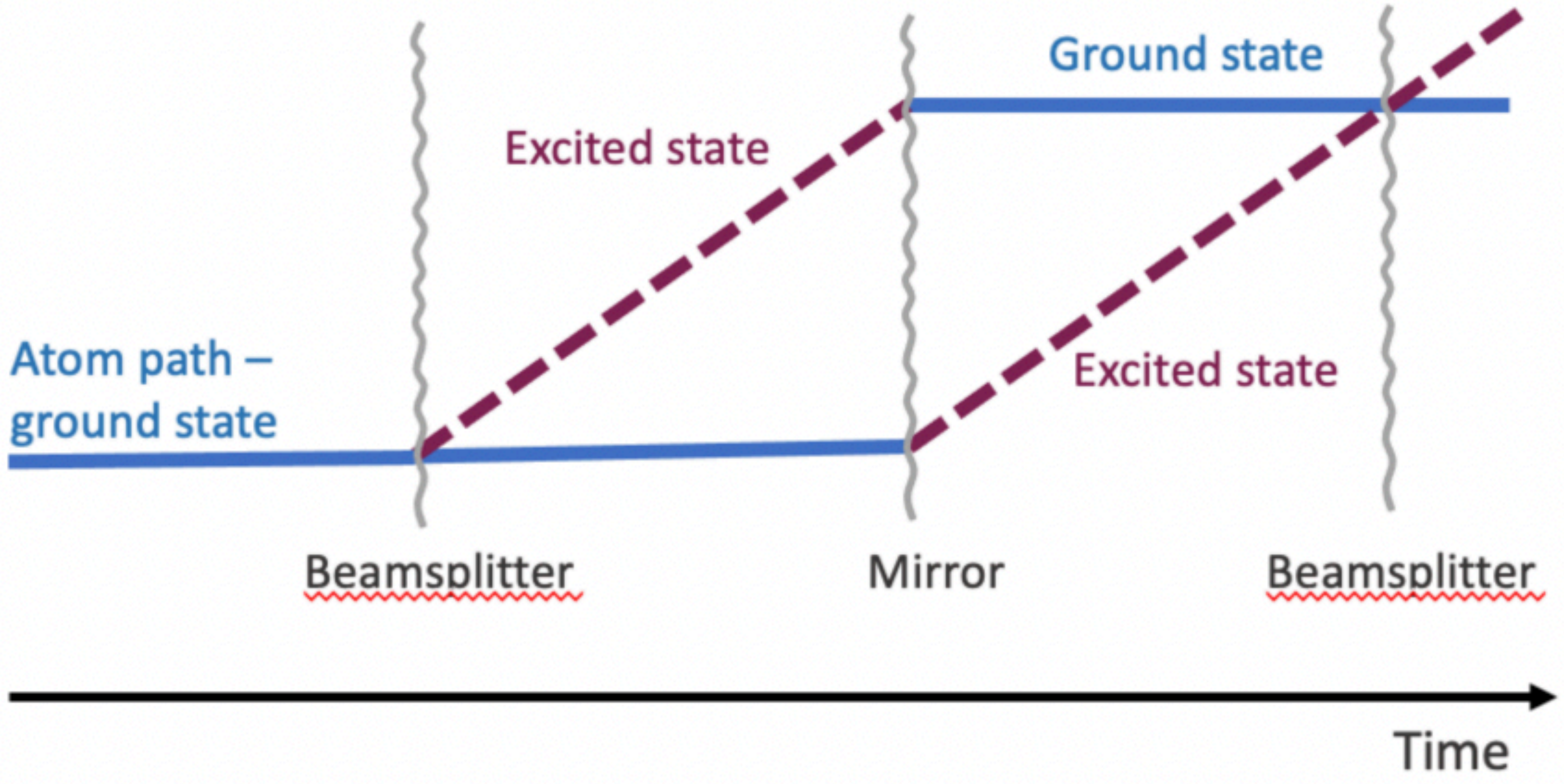

$$\omega_A(t,x) = \omega_A + \delta\omega_A(a)$$

$$\frac{\delta\omega_A(a)}{\omega_A} = \delta_e(a) + (2+\xi)\,\delta_\alpha(a)$$
$$\approx (\delta_e + (2+\xi)\delta_\alpha)\,\frac{\rho_{\rm DM}}{m_a^2 f^2}\cos(2\omega_a t) \equiv \overline{\omega}_A \cos(2\omega_a t)$$

$$\Phi_{t_1}^{t_2} = \int_{t_1}^{t_2} \delta\omega_A(a)dt$$

The total phase difference for a single AI is obtained by summing over all such paths in which the atom is in the excited state

Gradiometers

A system of two or more interferometers is used to cancel the common laser phase noise

separation between two AIs

$$\Phi_s = \frac{4\,\overline{\omega}_A}{\omega_a}\frac{\Delta r}{L}\sin\left(\omega_a n L\right)\sin\left(\omega_a T\right)\sin\{\omega_a\left(T+(n-1)L\right)\}$$

Baseline length

Interrogation time

Proposals

- Compact gradiometers : **AION-10 and MAGIS**
- Longer baselines - 100 m and km length baselines
- Space based - **AEDGE**

$$\Phi_s = 4\,\overline{\omega_a} n \Delta r \sin^2\left(m_a T\right)$$

- Longer baseline corresponds to higher sensitivity
- Low frequencies prone to gravity gradient noise

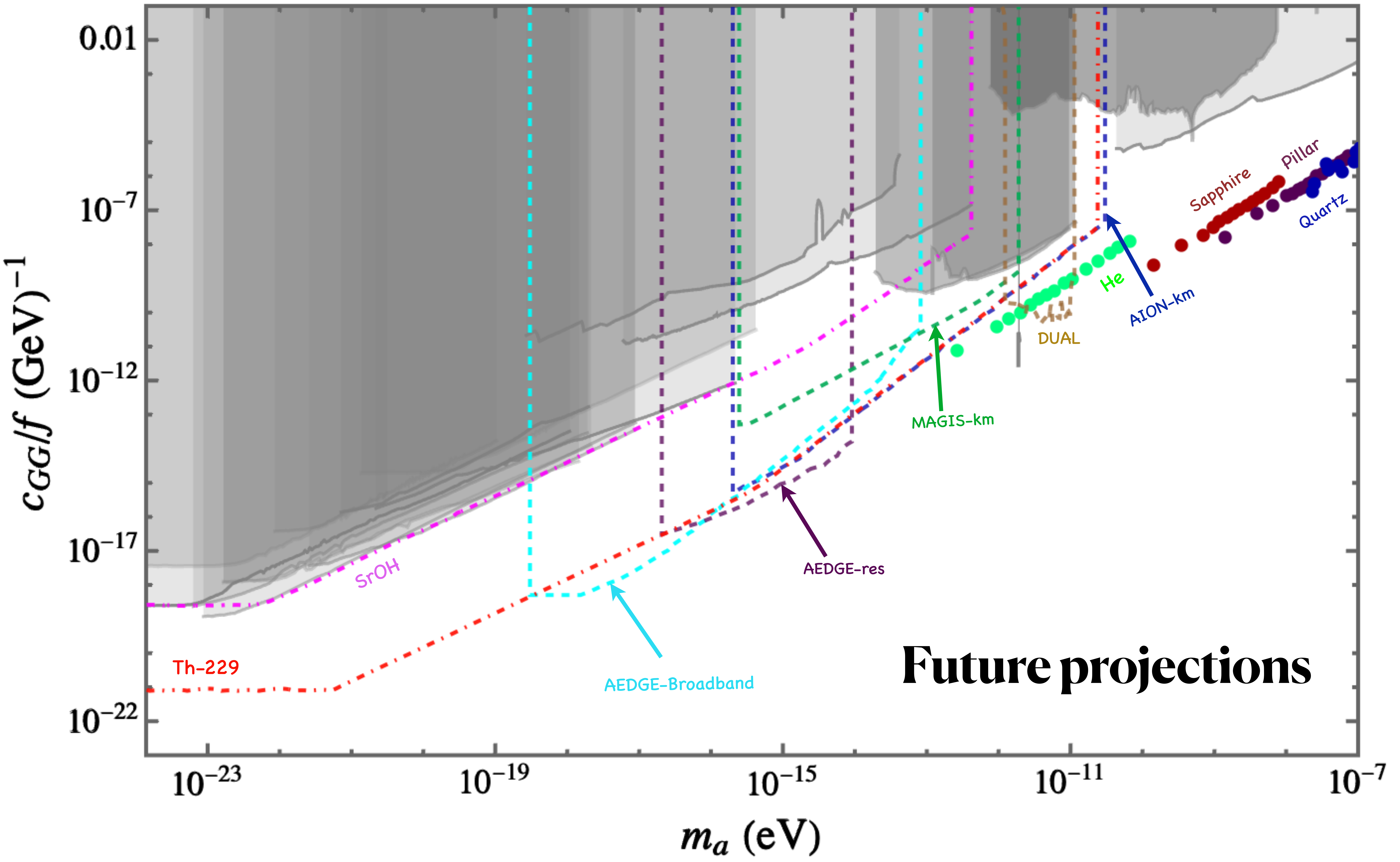

$c_{GG}/f\ (\mathrm{GeV})^{-1}$
0.01
10^{-7}
10^{-12}
10^{-17}
10^{-22}
10^{-23}
10^{-19}
10^{-15}
10^{-11}
10^{-7}
m_a (eV)
Sapphire
Pillar
Quartz
He
AION-km
DUAL
MAGIS-km
SrOH
AEDGE-res
Th-229
AEDGE-Broadband
Future projections

Putting everything together

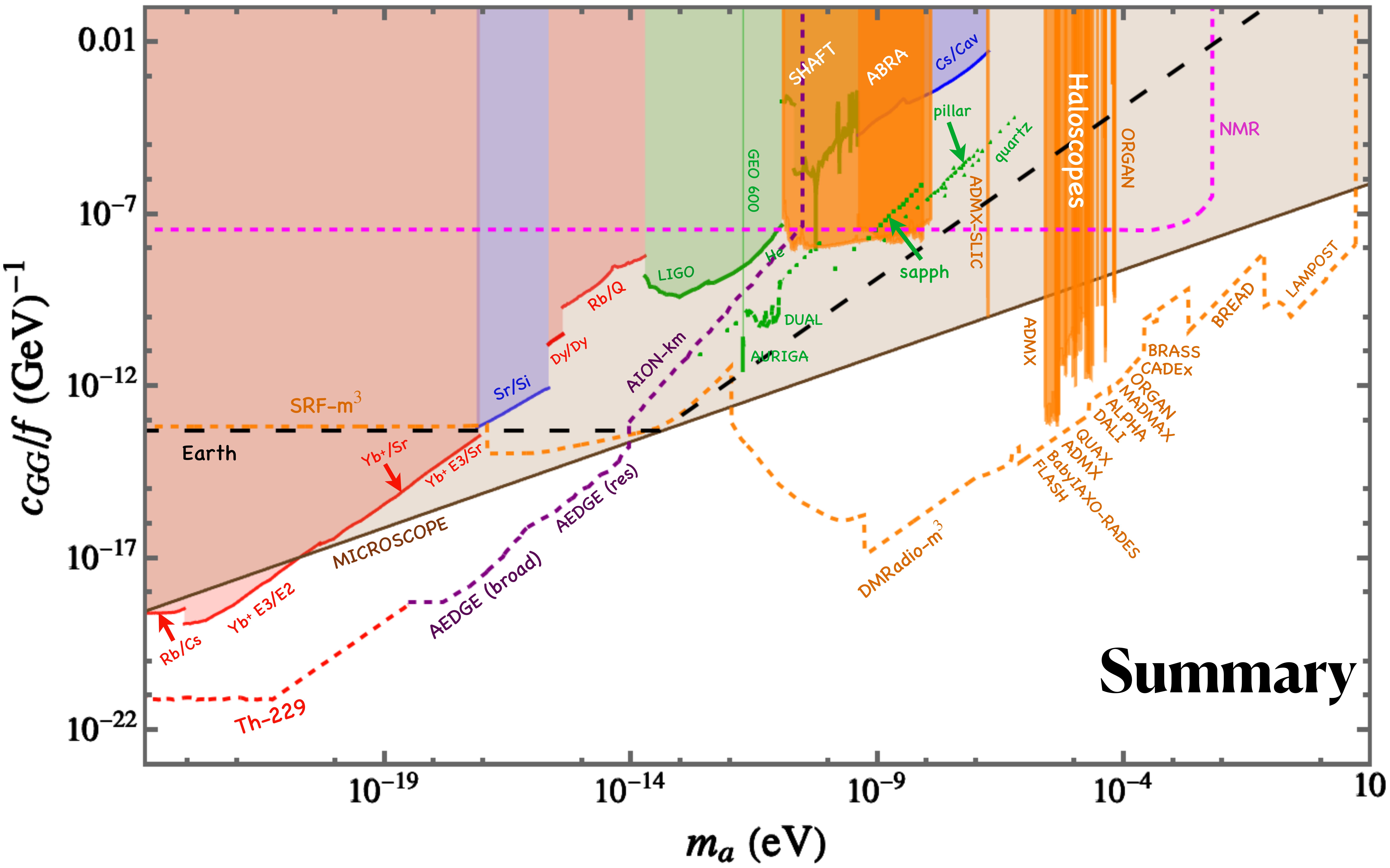

Summary
c_{GG}/f (GeV)$^{-1}$
m_a (eV)
0.01
10^{-7}
10^{-12}
10^{-17}
10^{-22}
10^{-19}
10^{-14}
10^{-9}
10^{-4}
10
SHAFT
ABRA
Cs/Cav
pillar
quartz
Haloscopes
ORGAN
NMR
GEO 600
ADMX-SLIC
sapph
He
LIGO
Rb/Q
Dy/Dy
DUAL
AURIGA
AION-km
Sr/Si
SRF-m^3
Earth
Yb+/Sr
Yb+ E3/Sr
MICROSCOPE
AEDGE (res)
AEDGE (broad)
Yb+ E3/E2
Rb/Cs
Th-229
ADMX
BRASS
CADEx
ORGAN
MADMAX
ALPHA
DALI
QUAX
ADMX
BabyIAXO-RADES
FLASH
BREAD
LAMPOST
DMRadio-m^3

Take home

- We consider ALPs coupled to only gluons at the UV scale.
- The gluon coupling at the UV scale induces various low-energy interactions, linear and quadratic
- Quadratic couplings induce ALP field-dependent shifts in the fundamental constants, which in the oscillating dark matter background, give rise to time-variations of these quantities.
- Quantum sensors probe quadratic couplings over a mass range $m_a \approx 10^{-24} - 10^{-6}\,\mathrm{eV}$
- Linear couplings are probed with haloscopes which are sensitive around $\mathcal{O}(\mu\mathrm{eV})$ range
- Upcoming quantum sensors provide very promising prospects in probing ultralight dark sectors.

Thank you!!

Finite density effects

Axion-field value is different in the vicinity of a massive object (such as the earth) than in the vacuum.

$$(\partial_t^2 - \Delta + m_a^2)a = -\sin\left(\frac{a}{f}\right)\sum_i \frac{Q_i^{\text{source}}\delta_i}{f}\rho_{\text{source}}(r)$$

$$= -\frac{a}{f}\sum_i \frac{Q_i^{\text{source}}\delta_i}{f}\rho_{\text{source}}(r) + \mathcal{O}\left(\frac{a^3}{f^3}\right)$$

The source term up to quadratic axion interactions can be absorbed in the effective mass term

$$\bar{m}_a^2(r) = m_a^2 + \sum_i \frac{Q_i^{\text{source}}\delta_i}{f^2}\rho_{\text{source}}(r)$$

$$(\partial_t^2 - \Delta + \bar{m}_a^2(r))a = 0\,.$$

$$a(t,r) = \frac{\sqrt{2\rho_{\text{DM}}}}{m_a}\cos(m_a t)\left[1 - Z_\delta J_\pm\big(\sqrt{3|Z_\delta|}\big)\frac{R_{\text{source}}}{r}\right]$$

axion field at infinity takes the oscillating galactic background field

$$a(t,r) = \frac{\sqrt{2\rho_{\rm DM}}}{m_a}\cos(m_a t)\left[1 - Z_\delta J_\pm\left(\sqrt{3|Z_\delta|}\right)\frac{R_{\rm source}}{r}\right]$$

$$Z_\delta = \frac{1}{4\pi f^2}\frac{M_{\rm source}}{R_{\rm source}}\sum_i Q_i^{\rm source}\delta_i$$

$$J_+(x) = \frac{3}{x^3}(x - \tanh x)\,,$$
$$J_-(x) = \frac{3}{x^3}(\tan x - x)\,.$$

$$Q_{\hat m} = \left[9.3 - \frac{3.6}{A^{1/3}} - 2\frac{(A-2Z)^2}{A^2} - 0.014\frac{Z(Z-1)}{A^{4/3}}\right]\times 10^{-2};$$
$$Q_{\Delta M} = 1.7\times 10^{-3}\frac{A-2Z}{A}\,,$$
$$Q_\alpha = \left[-1.4 + 8.2\frac{Z}{A} + 7.7\frac{Z(Z-1)}{A^{4/3}}\right]\times 10^{-4}\,,$$
$$Q_e = 5.5\times 10^{-4}\frac{Z}{A}\,,$$

Damour, Donoghue, et. al

$$\delta_\pi = -2c_{GG}^2\frac{m_u m_d}{(m_u+m_d)^2}$$

$$\delta_N = -4c_1\frac{m_\pi^2}{M_N}\delta_\pi,$$
$$\delta_{\Delta M} = \delta_\pi\,,$$
$$\delta_\alpha = \frac{1}{12\pi}\left(1 - 32c_1\frac{m_\pi^2}{M_N}\right)\delta_\pi\,,$$
$$\delta_e = \frac{\alpha}{16\pi^2}\ln\frac{m_e^2}{m_\pi^2}\left(1 - 32c_1\frac{m_\pi^2}{M_N}\right)\delta_\pi$$

Q_i's are positive, δ_i's are negative

$J\_(x)$ diverges for $x \to \pi/2$

$$\frac{c_{GG}}{f} \gtrsim \left(\frac{6}{\pi^3}\frac{m_u m_d}{(m_u+m_d)^2}\frac{M_\oplus}{R_\oplus}|Q_{\hat m}|\right)^{-1/2} \approx \frac{1}{10^{15}}\,{\rm GeV}^{-1}$$

critical value of the axion-gluon coupling under the small-coupling approximation

- Axion potential is periodic, resulting in a cutoff for the field value $a \sim \pi/f$, implying that the higher order operators in the expansion regulates the divergence in the field.
- For non-DM axion, the boundary condition at $r \to \infty$ is a vanishing field value, so the full solution can be obtained. In the case of axion dark matter it should be finite as the free oscillating field - **Needs proper treatment**

$$V = -m_\pi^2 f_\pi^2 \epsilon \sqrt{1 - \frac{4 m_u m_d}{(m_u + m_d)^2} \sin^2\left(\frac{a}{2 f_a}\right)}.$$

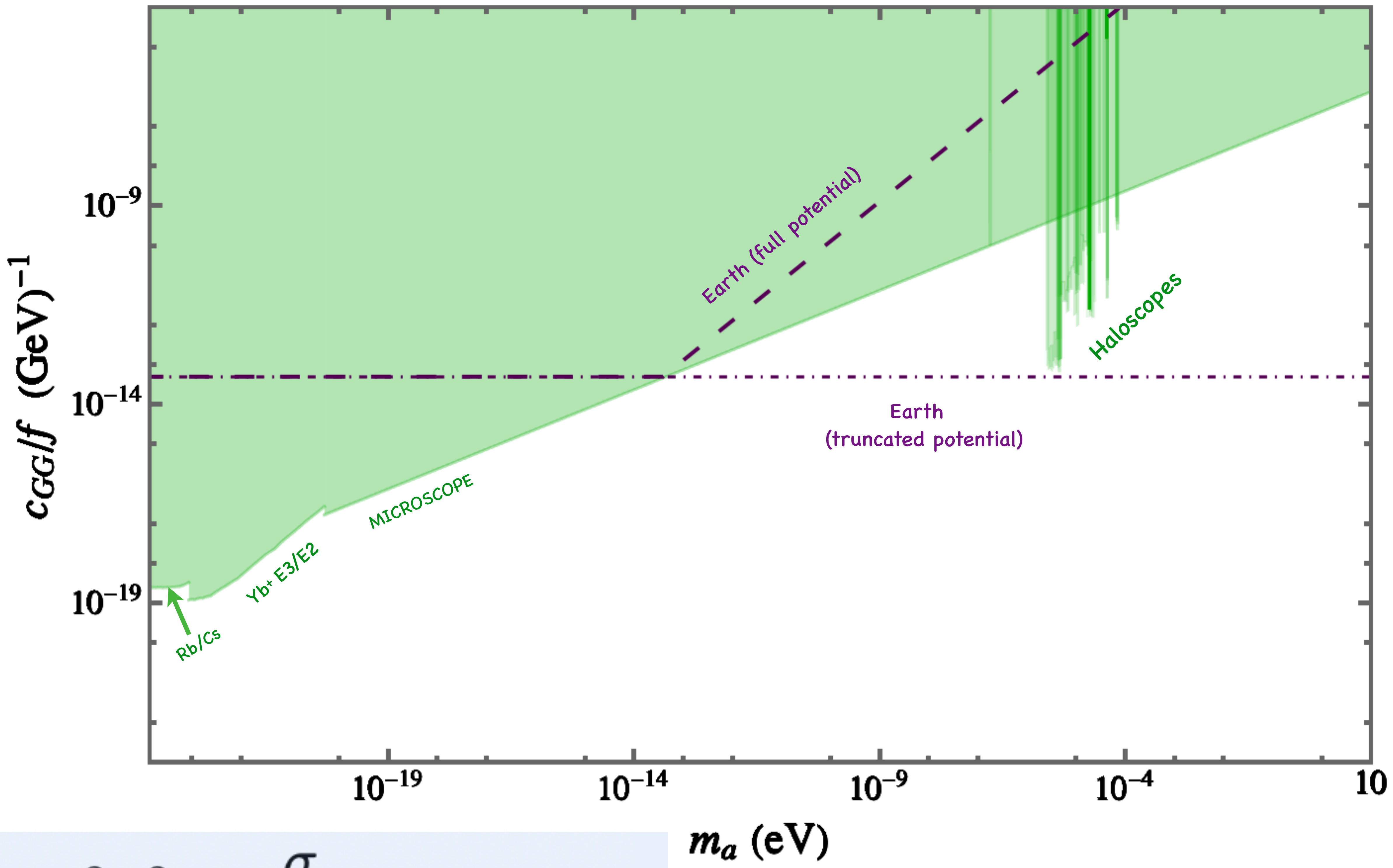

For the axion field value to deviate from the vacuum solution, the potential energy induced by the source needs to be **sufficiently large** to turn the axion mass tachyonic

$$m_a^2 f^2 + \frac{\sigma}{M_N} \rho_N \, \delta_\pi < 0 \,,$$

$$m_a^2 f^2 < 5 \times 10^{17} \, c_{GG}^2 \, \mathrm{eV}^4$$

Non-dark matter axions

Hook and Huang et. al, 1708.08464

vacuum solution, $\langle a \rangle = 0$ $\quad$ $\boxed{m_a \sim m_\pi f_\pi / f_a}$

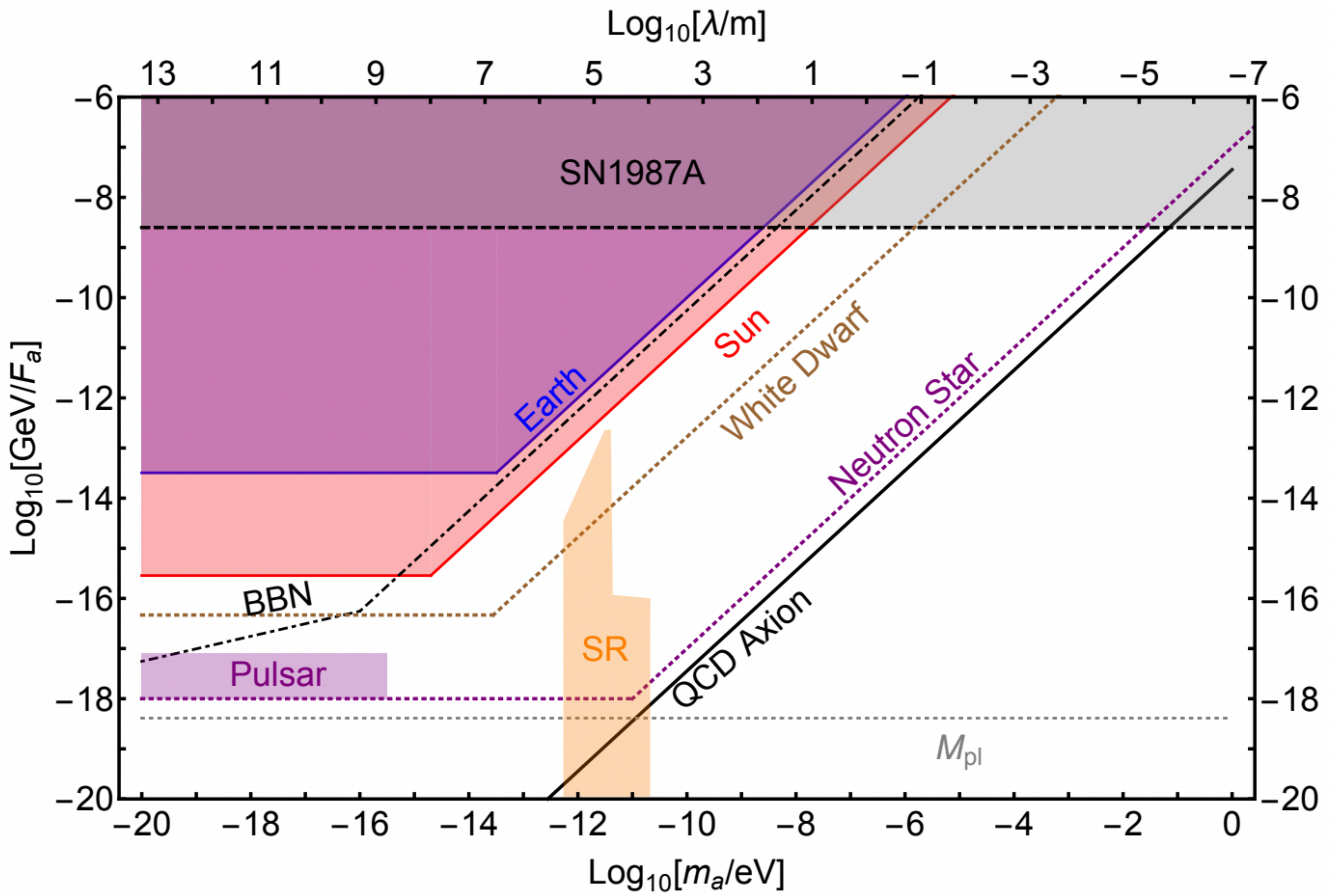

$$V = -m_\pi^2 f_\pi^2 \left\{ \left(\epsilon - \frac{\sigma_N n_N}{m_\pi^2 f_\pi^2} \right) \left| \cos\left(\frac{a}{f_a} \right) \right| + \mathcal{O}\left(\left(\frac{\sigma_N n_N}{m_\pi^2 f_\pi^2} \right)^2 \right) \right\}$$

In a dense medium

$$\sigma_N \equiv \sum_{q=u,d} m_q \frac{\partial m_N}{\partial m_q},$$

- gradient energy required to move the axion away from $a = 0$ $\sim \left(f_a^2 / r^2 \right)$
- when the energy from the finite density effects overcomes the mass, the minimum of the potential shifts to π
- when the gain in potential energy outweighs the gradient energy, the axion gets sourced by the finite density medium

$$r_{\text{crit}} \gtrsim \frac{1}{m_T}, \qquad m_T = m_\pi f_\pi \frac{\sqrt{\frac{\sigma_N n_N}{m_\pi^2 f_\pi^2} - \epsilon}}{2 f_a}$$

Axions and ALPs

- QCD Axion : a solution to the strong CP problem - $\theta_{\text{QCD}} \propto a/f_a$ ✓
  Peccei Quinn 1972, Weinberg 1978, Wilczek 1978
- $m_a \propto \Lambda^2_{\text{QCD}}/f_a$ - mass related to the interactions with SM particles ✓
- Pseudo Nambu-Goldstone bosons : has derivative couplings - $\partial_\mu a \bar{\psi} \gamma_5 \psi / f_a$ ✓
- Can constitute a component or all of cold dark matter ✓

Axions and ALPs

- ~~QCD Axion : a solution to the strong CP problem -~~ $\cancel{\theta_{\mathrm{QCD}} \propto a/f_a}$ Axion-like particles (ALPs) do not solve strong CP
- $\cancel{m_a \propto \Lambda^2_{\mathrm{QCD}}/f_a}$ ~~- mass related to the interactions with SM particles~~ ALP mass is a free parameter
- Pseudo Nambu-Goldstone bosons : has derivative couplings - $\partial_\mu a \, \bar{\psi}\gamma_5\psi/f_a$
- Can constitute a component or all of cold dark matter

Pions

$$\mathcal{L}_{\chi \mathrm{PT}} = \frac{f_\pi^2}{4}\mathrm{tr}[\Sigma m_q(a)^\dagger + m_q(a)\Sigma^\dagger] + \ldots \,,$$

where $\Sigma = \exp\left(i\sqrt{2}\Pi/f_\pi\right)$ and the quark mass matrix is ALP-field dependent

$$m_q(a) = e^{-i\kappa_q \frac{a}{f} c_{GG}} m_q e^{-i\kappa_q \frac{a}{f} c_{GG}},$$

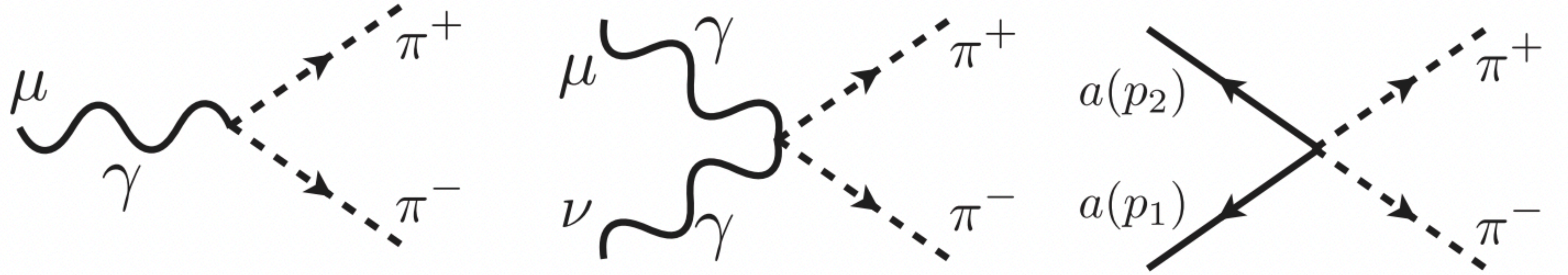

$-i\,e\,(p_+ - p_-)_\mu$ $\quad$ $2\,i\,e^2\,g_{\mu\nu}$ $\quad$ $\frac{i}{f_a^2}\left[\frac{m_u\,m_d\,m_\pi^2}{(m_u+m_d)^2} - \frac{2(m_d-m_u)^2 p_1\cdot p_2}{(m_u+m_d)^2}\right]$

Feynman rules for the vertices from the $\mathcal{O}(p^2)$ chiral Lagrangian leading to a loop-induced a^2F^2 coupling.

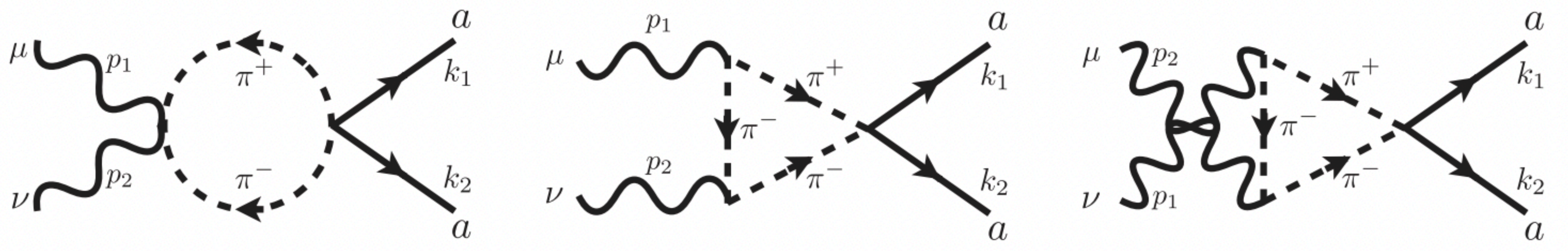

Three diagrams contributing to $\gamma\gamma \to aa$ at $\mathcal{O}(p^4)$ in the χPT Lagrangian.

C. Beadle et. al : PhysRevD.110.035019

Nucleons

$$\mathcal{L}_{\chi\mathrm{PT}}^{(2)} = c_1 \mathrm{tr}[\chi_+]\bar{N}N + \ldots\ ,$$

$$\chi_+ = 2B_0\big(\xi^\dagger m_q(a)\xi^\dagger + \xi m_q^\dagger(a)\xi\big)$$

$$M_N = M_0 - 4c_1 m_\pi^2$$

$$c_1 \mathrm{tr}[\chi_+]\bar{N}N = C_N \frac{a^2}{f^2}\bar{N}N + \ldots = 4c_1 m_\pi^2\, \delta_\pi(a)\bar{N}N + \ldots$$

New developments in optical clocks

The QCD-interactions of the oscillating dark matter field give rise to oscillations in the nuclear charge radius. In heavy atoms like $^{171}\mathrm{Yb}^+$, there is a large contribution from the "field-shift energy" in the total electronic energy, since $E_{\mathrm{FS}} \simeq K_{\mathrm{FS}} \langle r_N^2 \rangle \propto A^{2/3}$.

$$\frac{\Delta(\nu_a/\nu_b)}{(\nu_a/\nu_b)} = K_{a,b} \frac{\Delta \langle r_N^2 \rangle}{\langle r_N^2 \rangle} \qquad K_{a,b} \equiv \frac{K_{\mathrm{FS}}^{\nu_a} \langle r_N^2 \rangle}{\nu_a} - \frac{K_{\mathrm{FS}}^{\nu_b} \langle r_N^2 \rangle}{\nu_b}$$

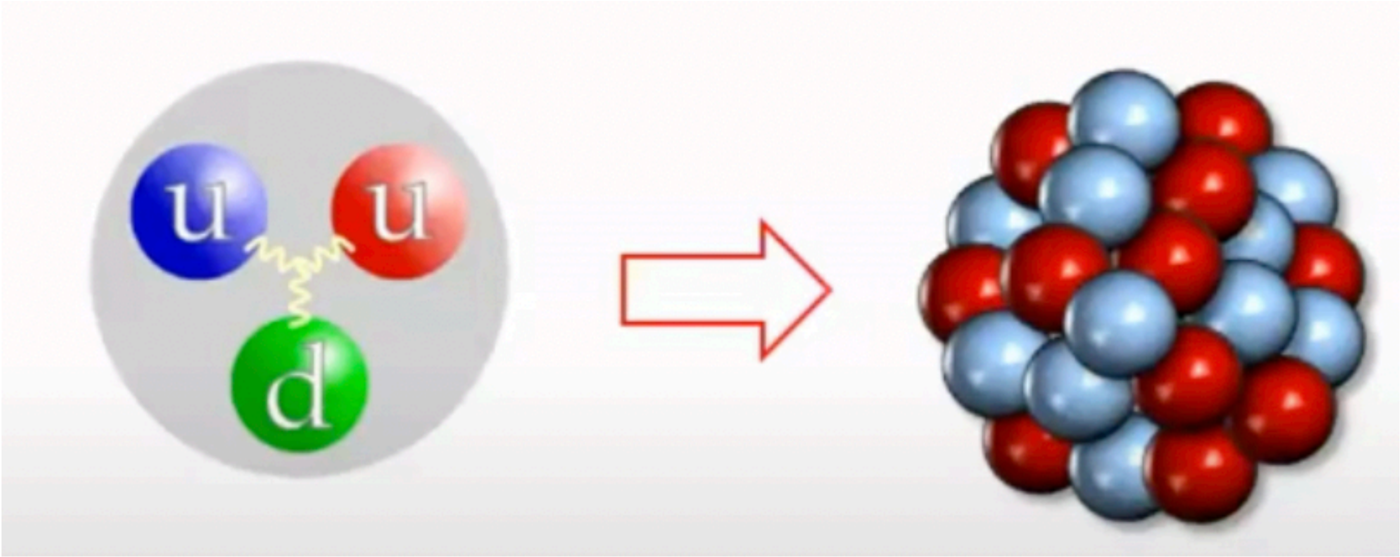

courtesy : M. Safronova

$\langle r_N^2 \rangle$ is dominated by the distribution of protons within the nucleus and the inter-nucleon distance, which are sensitive to pion decay constant, pion mass and pion-exchange processes.

$$\frac{\Delta \langle r_N^2 \rangle}{\langle r_N^2 \rangle} \approx \alpha \frac{\Delta f_\pi}{f_\pi} + \beta \frac{\Delta m_\pi^2}{m_\pi^2} \approx \alpha \frac{\Delta \Lambda_{\mathrm{QCD}}}{\Lambda_{\mathrm{QCD}}} + \beta \frac{\Delta m_\pi^2}{m_\pi^2}$$

sensitivity improved by several orders compared to BACON clocks!!

Yb^+ $\mathrm{E}_3/\mathrm{E}_2$

$(4f^{14}6s)^2S_{1/2} - (4f^{13}6s)^2F_{1/2}$ (E_3)

$(4f^{14}6s)^2S_{1/2} - (4f^{14}5d)^2D_{3/2}$ (E_2)

`Banerjee et.al,arXiv:2301.10784`

Heavier ALP mass

ADMX-SIDECAR, ORGAN - tunable to higher cavity modes

Future proposals

..And many more !!

Non-DM ALP landscape